

Award Number: W81XWH-10-1-0008

TITLE: Stationary Digital Tomosynthesis System for Early Detection of Breast Tumors

PRINCIPAL INVESTIGATOR: Xin Qian

CONTRACTING ORGANIZATION: University of North Carolina at Chapel Hill
Chapel Hill, NC 27599

REPORT DATE: May 2012

TYPE OF REPORT: Annual Summary

PREPARED FOR: U.S. Army Medical Research and Materiel Command
Fort Detrick, Maryland 21702-5012

DISTRIBUTION STATEMENT: Approved for public release; distribution unlimited

The views, opinions and/or findings contained in this report are those of the author(s) and should not be construed as an official Department of the Army position, policy or decision unless so designated by other documentation.

REPORT DOCUMENTATION PAGE

Form Approved
OMB No. 0704-0188

Public reporting burden for this collection of information is estimated to average 1 hour per response, including the time for reviewing instructions, searching existing data sources, gathering and maintaining the data needed, and completing and reviewing this collection of information. Send comments regarding this burden estimate or any other aspect of this collection of information, including suggestions for reducing this burden to Department of Defense, Washington Headquarters Services, Directorate for Information Operations and Reports (0704-0188), 1215 Jefferson Davis Highway, Suite 1204, Arlington, VA 22202-4302. Respondents should be aware that notwithstanding any other provision of law, no person shall be subject to any penalty for failing to comply with a collection of information if it does not display a currently valid OMB control number. **PLEASE DO NOT RETURN YOUR FORM TO THE ABOVE ADDRESS.**

1. REPORT DATE (DD-MM-YYYY) 01-05-2012		2. REPORT TYPE Annual Summary		3. DATES COVERED (From - To) 1 MAY 2011 - 30 APR 2012	
4. TITLE AND SUBTITLE Stationary Digital Tomosynthesis System for Early Detection of Breast Tumors				5a. CONTRACT NUMBER	
				5b. GRANT NUMBER W81XWH-10-1-0008	
				5c. PROGRAM ELEMENT NUMBER	
6. AUTHOR(S) Xin Qian E-Mail: qianx2006@gmail.com				5d. PROJECT NUMBER	
				5e. TASK NUMBER	
				5f. WORK UNIT NUMBER	
7. PERFORMING ORGANIZATION NAME(S) AND ADDRESS(ES) University of North Carolina at Chapel Hill Chapel Hill, NC 27599				8. PERFORMING ORGANIZATION REPORT NUMBER	
9. SPONSORING / MONITORING AGENCY NAME(S) AND ADDRESS(ES) U.S. Army Medical Research and Materiel Command Fort Detrick, Maryland 21702-5012				10. SPONSOR/MONITOR'S ACRONYM(S)	
				11. SPONSOR/MONITOR'S REPORT NUMBER(S)	
12. DISTRIBUTION / AVAILABILITY STATEMENT Approved for Public Release; Distribution Unlimited					
13. SUPPLEMENTARY NOTES					
14. ABSTRACT Stable operation of the new developed s-DBT scanner at 28kVp anode voltage and 38mA tube current was demonstrated with extended lifetime and good source-to-source consistency. For standard imaging protocol of 15 views, 14 degree, 100mAs dose, and 2x2 detector binning the projection resolution along scanning direction is increased from 4.0 lps/mm (at 10% MTF) in DBT to 5.1 lps/mm in s-DBT at magnification factor of 1.1. The improvement is more pronounced for faster scanning speed, wider angular coverage, and smaller detector pixel size. The scanning speed depends on the detector, the number of views, and the imaging dose. With 240ms detector readout time the s-DBT system scanning time is 6.3s for a 15-view, 100mAs scan regardless of the angular coverage. The scanning speed can be reduced to less than 4s when detectors become faster. Initial phantom studies showed good quality reconstructed images.					
15. SUBJECT TERMS breast cancer, x-ray, digital breast tomosynthesis					
16. SECURITY CLASSIFICATION OF:			17. LIMITATION OF ABSTRACT	18. NUMBER OF PAGES	19a. NAME OF RESPONSIBLE PERSON
a. REPORT	b. ABSTRACT	c. THIS PAGE			19b. TELEPHONE NUMBER (include area code)
U	U	U	UU	68	USAMRMC

Table of Contents

	<u>Page</u>
Introduction.....	2
Body.....	3
Key Research Accomplishments.....	16
Reportable Outcomes.....	18
Conclusion.....	19
References.....	20
Appendices.....	21

Introduction

Breast cancer is the most common type of cancer occurring in women. Early detection is considered as the best hope for decreasing the mortality rate from breast cancer [1-4]. Digital breast tomosynthesis (DBT) has the potential to improve the effectiveness of early breast cancer screening at a similar dose and comparable cost as the full-field digital mammography (FFDM) [5]. There are however two important limitations of the current DBT technology: low spatial resolution and long scanning time comparing to FFDM. Both result directly from the limitations of the conventional x-ray tube technology where x-ray radiation is generated from a single focal spot and the flux is constrained by the anode heat load. Image blurring due to both source and patient motion is a major factor that degrades the spatial resolution of DBT and its sensitivity for small micro-calcifications (MC) compared to FFDM [6]. Although results from phantoms [7, 8] and clinical tests [9] have shown a higher sensitivity for mass compared to mammography, DBT by itself is often inferior to diagnostic mammography in characterization of MC [10], which is critical for diagnosis of cancer [11-13]. The Hologic Selenia DBT scanner was recently approved by FDA [14] to operate in the combo mode requiring acquisition of both 2D mammography and 3D tomosynthesis images for each patient to achieve good MC and mass detection. This however increases the total imaging dose [15].

To address the limitations of the current DBT technology, we recently developed a stationary digital breast tomosynthesis (s-DBT) in a bench top system using a vacuum chamber based CNT x-ray source array [16]. In particular we investigated the feasibility of improving the spatial resolution of the Hologic Selenia Dimensions DBT scanner by replacing the standard mammography x-ray tube with a specially designed distributed CNT source array. The aim is to increase the detection sensitivity of tomosynthesis for MC's to potentially eliminate the need for additional 2D mammography imaging. We further evaluated the scanning time at the targeted spatial resolution for a given set of detector readout times. The lifetime and consistency of the CNT x-ray source array were also tested.

Body

Task 1. Design and construct a fully functional full-field s-DBT scanner with the specially designed high-power MBFEX source (Months 1-17)

In order to perform a realistic comparison of performance, the configuration of the scanner is similar to the Hologic Selenia Dimensions scanner. The following specific works have been carried out in year two:

1.2 Manufacture the MBFEX source based on the specifications defined in 1.1. (Months 7-15)

1.2.3 X-ray tube fabrication: The MBFEX source will be made at UNC. The tube manufacturing and process work will be done at XinRay, Siemens is one of its two parent companies. The tube will have an open design with a flange that can be opened and re-closed. Therefore, the internal structure of x-ray source including the anode and the cathode array can be easily changed. (Months 9-15)

The electron source arrays have been fabricated at XinRay's facility in RTP, NC. The tube manufacturing and process work has been done at Siemens Medical Solution's, one of its parent companies, facilities in Germany.

Figure 1 shows the CNT x-ray source array designed for s-DBT. The tube contains an extended anode plate with 31 individual tungsten anodes and a two-stage active focusing assembly for electron beam focusing. In the picture one can see the main housing components consist of the HV feed-through for the anode voltage input, two ion getter pumps that allow the monitoring of the pressure inside the tube, and the large x-ray window made from Aluminum. The backside contains the electrical feed-through for the cathodes and the focusing electrodes. The tube was designed to provide similar scan modes as conventional moving source systems. The target material is tungsten in combination with a 1mm Aluminum filtration from the x-ray window. Additional filters and collimators can be installed on the tube housing.

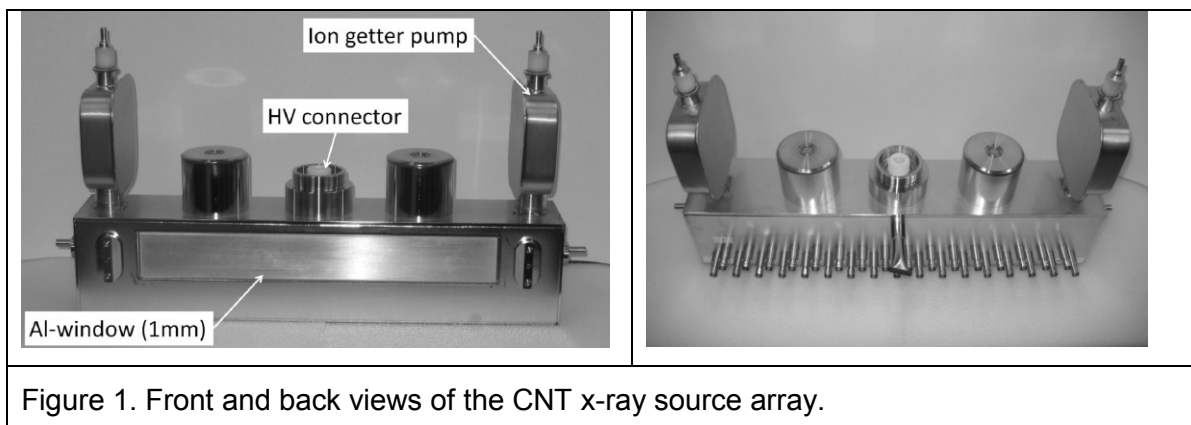


Figure 1. Front and back views of the CNT x-ray source array.

1.3 System integration: After the x-ray tube is delivered to UNC, the s-DBT system will be assembled. The whole system will be housed in an enclosure with x-ray shielding and safety inter-locks. (Months 16-17)

This specific work has been achieved.

The CNT x-ray source array was mounted on the rotating gantry of the Hologic Selenia

Dimensions scanner replacing its mammography x-ray tube, as illustrated in Figure 2. A mounting bracket was designed to connect the source array with the gantry and to provide multiple degrees of translational and rotational freedom to adjust the exact location and orientation of the source with respect to the detector plane. The x-ray source array was electronically interfaced with the Selenia detection unit which sets the number of views, the detector integration time, and the detector readout time. The x-ray source exposure time for each view is controlled by the x-ray control unit (XCU). The XCU also controls the current and sequence of the x-ray beams. The pulse width was programmed equal to the detector integration time. A TTL trigger signal from the Selenia detector unit to the XCU synchronizes the x-ray beam activation with the detector integration and readout. The XCU receives a separate trigger pulse from the detector unit for each exposure. During the scan

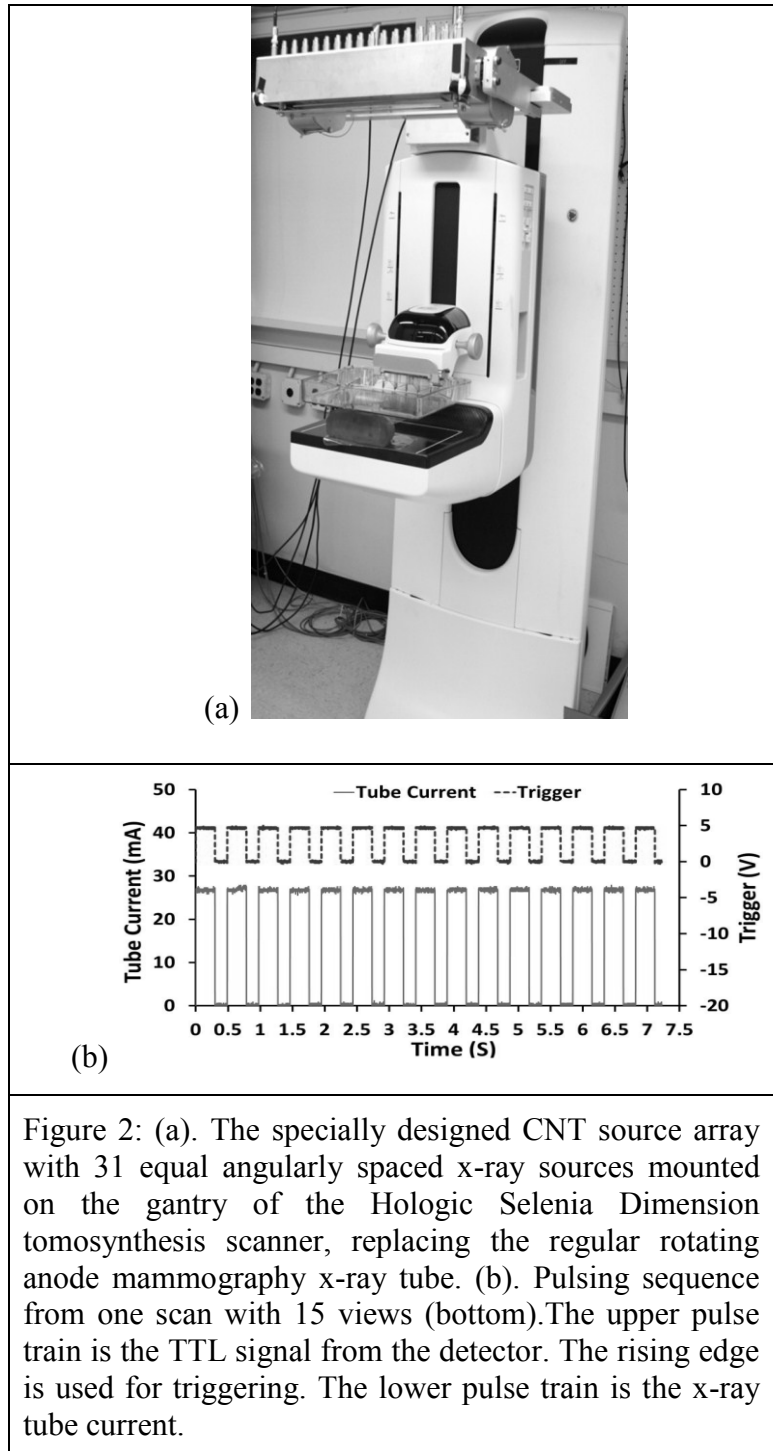


Figure 2: (a). The specially designed CNT source array with 31 equal angularly spaced x-ray sources mounted on the gantry of the Hologic Selenia Dimension tomosynthesis scanner, replacing the regular rotating anode mammography x-ray tube. (b). Pulsing sequence from one scan with 15 views (bottom). The upper pulse train is the TTL signal from the detector. The rising edge is used for triggering. The lower pulse train is the x-ray tube current.

sequence the XCU regulates the extraction voltage for the CNT cathodes to provide the programmed emission current value for each source.

Figure 2 shows an example from one tomosynthesis scan. The detector sent a TTL pulse train signal where each pulse corresponds to one detector frame with pre-set integration and readout time. The rising edge of each pulse triggers exposure from one corresponding x-ray source where the x-ray pulse width is programmed to be the same as the detector integration time. The amplitude of the CNT cathode current, therefore the x-ray tube current, is regulated by the XCU which automatically varies the extraction voltage applied to achieve the targeted value which can either be the same for each source or varies in a pre-programmed pattern.

Task 2 Evaluate the system performance using phantoms and compare the new system with commercial prototype DBT scanners (Months 18-28)

The aim is to compare the new developed s-DBT scanner with the original Hologic Selenia Dimensions scanner in terms of focal spot size, modulation transfer function, and image quality using standard phantoms. The following specific works have been carried out in year two:

2.1 Fully calibrate the performance of the MBFEX source: a).The energy distribution of the MBFEX source; b).The tube current as a function of time at different gate voltages; c).Detect the generated x-ray radiation and test the electronics circuit; d). Measure the x-ray focal spot size following the industrial standard. Any pixel-to-pixel variation in the focal spot size will be corrected by varying the potential of the focusing electrodes; e).Find the spatial resolution of the system using the modulation transfer function (MTF) phantom; f).Geometry calibration will be performed based on identification of ellipse parameters; g).Dose measurements will be supervised by our collaborator Pisano in the department of Radiology at UNC. (Months 18-22)

These specific tasks have been achieved.

a) The energy distribution of the MBFEX source

X-ray intensity distribution was measured at 28kVp, 10 mAs, 70cm source to detector distance. No additional filter was used except the 1mm thick Al window. The line profiles of intensity values in the region of interest on the detector were plotted.

Figure 3 shows the x-ray intensity within the 130mmx90mm region of interest (ROI) recorded on the detector (2x2 binning) using the center x-ray beam. The x-ray intensity variation for the horizontal line is 5% and 4% in the vertical direction. The same measurement was performed for all 31 x-ray beams. The percentage variation of intensity is 4%- 9% for all 31 x-ray beams. The variation is larger outside of the ROI.

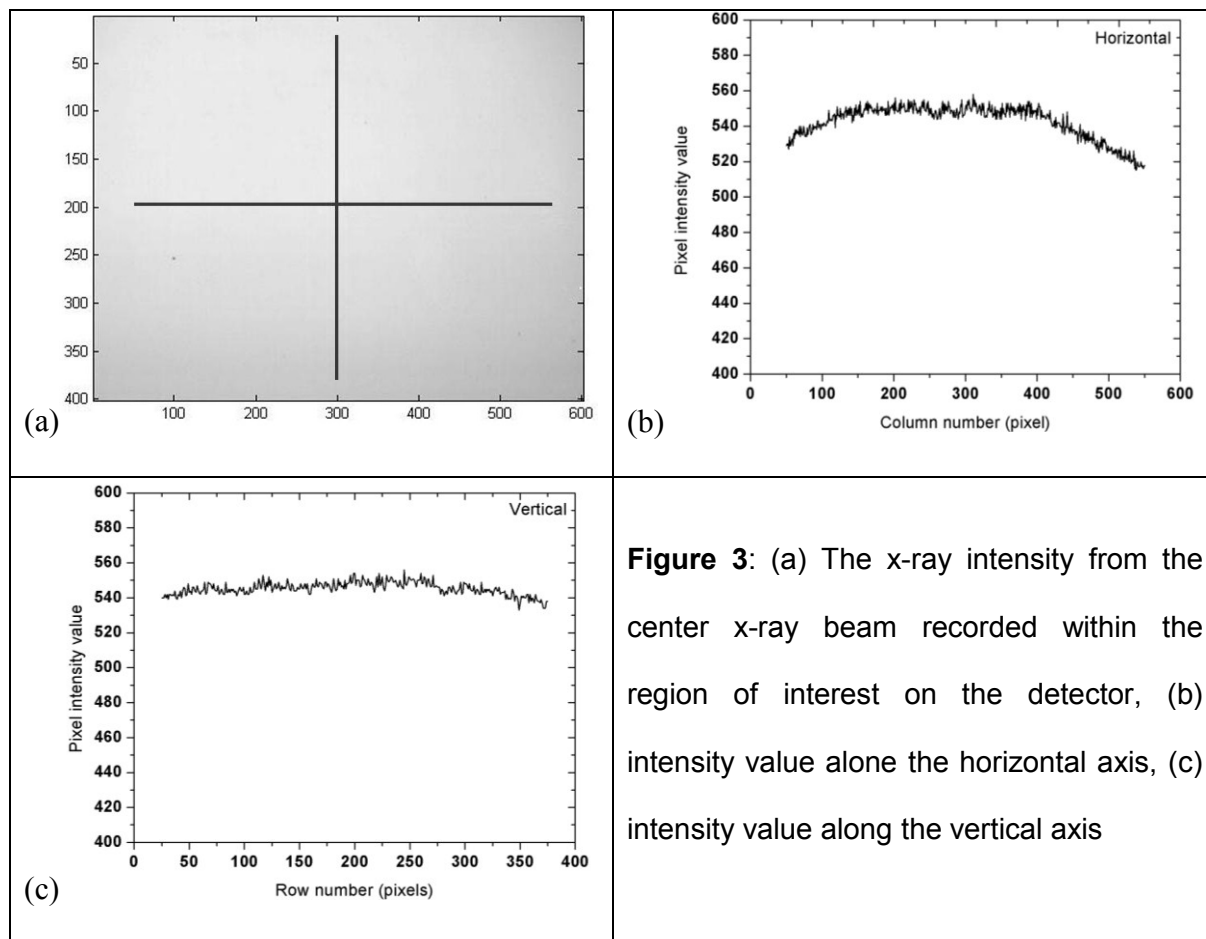


Figure 3: (a) The x-ray intensity from the center x-ray beam recorded within the region of interest on the detector, (b) intensity value along the horizontal axis, (c) intensity value along the vertical axis

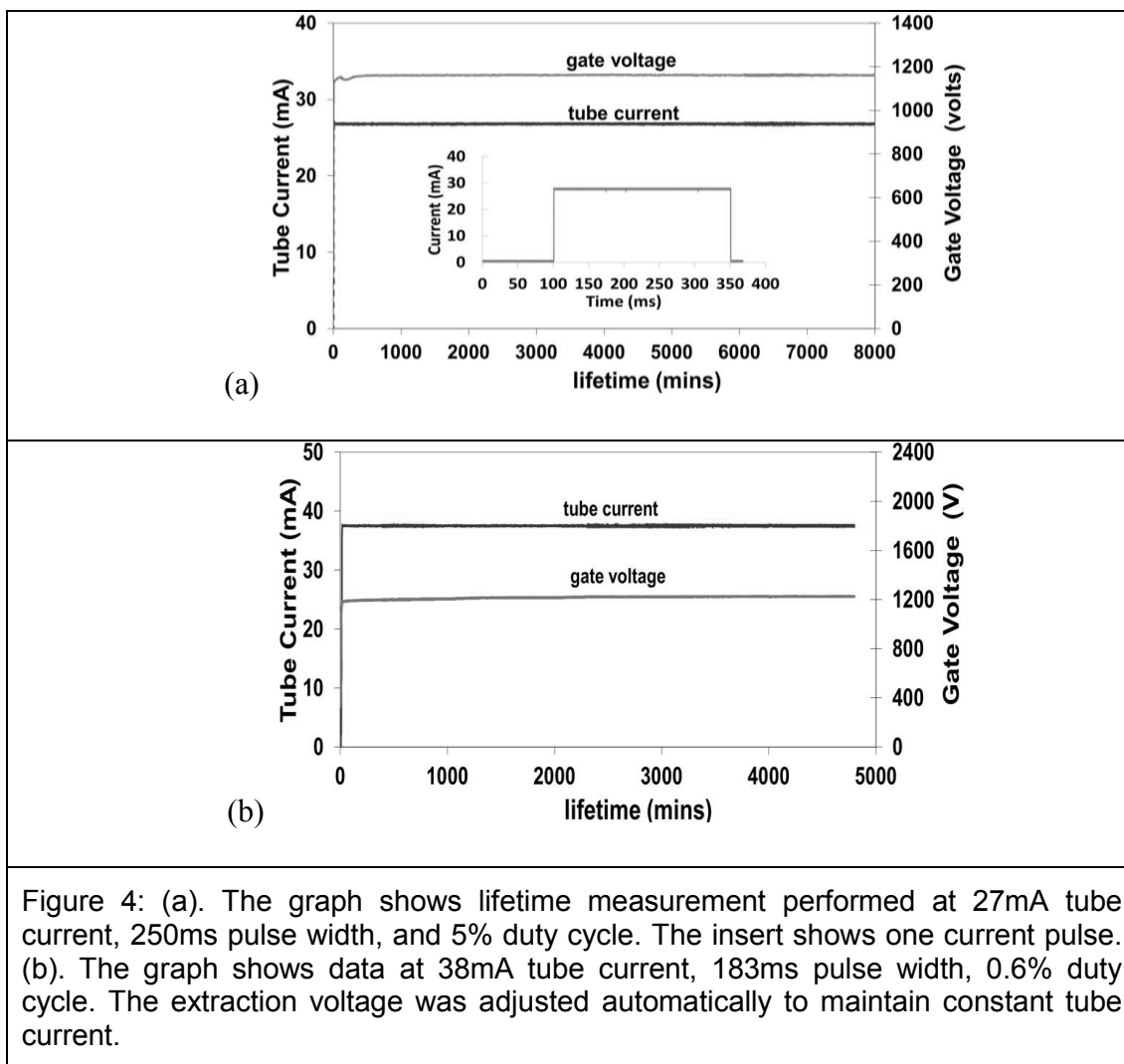
b) The tube current as a function of time at different gate voltages

Several factors considered in designing the CNT cathode include the targeted focal spot size, the demagnification factor of the electrostatic lens, the anode tilting angle, and the maximum stable emission current density of the CNT emitters. The aim of the present study is to have an isotropic focal spot size of $\sim 0.6\text{mm} \times 0.6\text{mm}$ FWHM which will provide a significant improvement in the spatial resolution along the scanning direction while maintaining a comparable value in the direction orthogonal to motion. The basic structure of each x-ray unit (source) consists of a CNT cathode, a gate electrode to extract electrons, electron focusing lens, and the anode. To focus the field emitted electron beam the modified Einzel-type electrostatic lens described in our previous publications was utilized.

The emission current from the CNT cathode was evaluated using anticipated operating conditions before the x-ray tube was manufactured with use of a vacuum chamber based test module housing 3 x-ray sources. The test module has a similar structure as the designed tube, with each source consisting of a CNT cathode, an extraction gate, focusing lens, and a W anode. Accelerated lifetime measurements were performed under the pulse mode with variable pulse width and duty cycle. Each pulse corresponds to one x-ray exposure. Long term stability

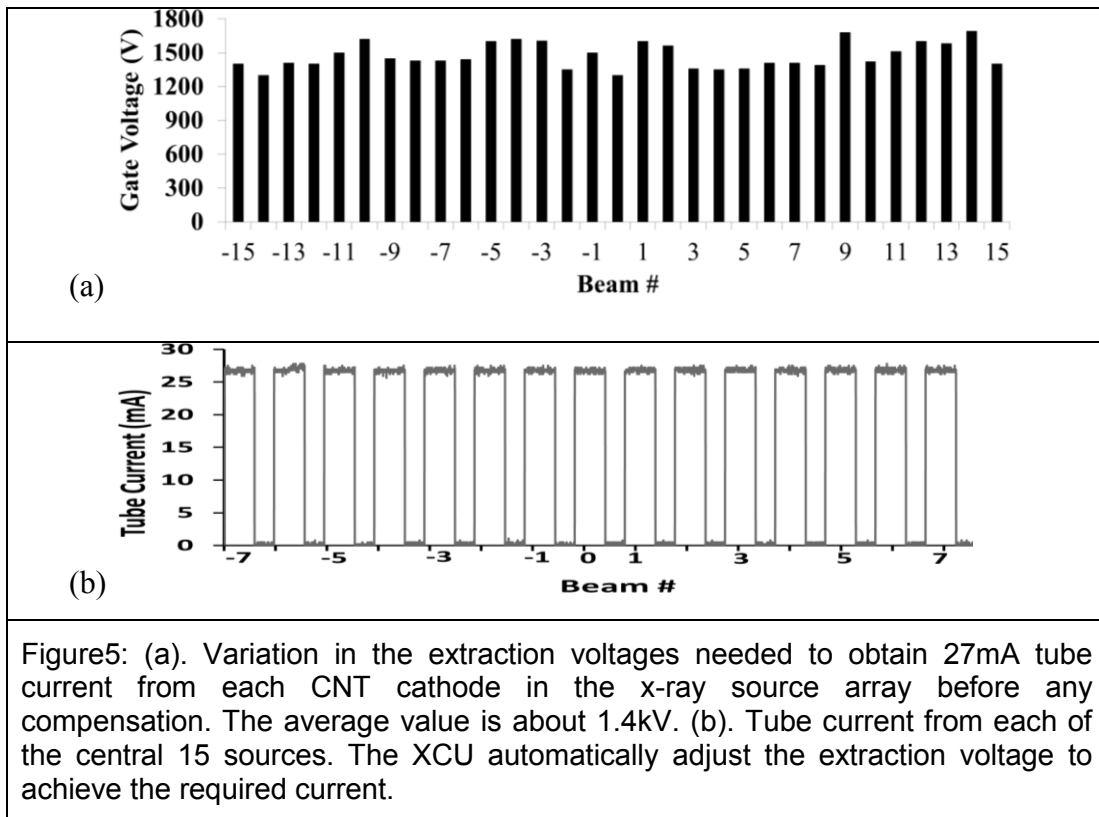
was tested for 250ms and 183ms pulses. During the measurement the extraction electrical field was automatically adjusted to maintain a constant current.

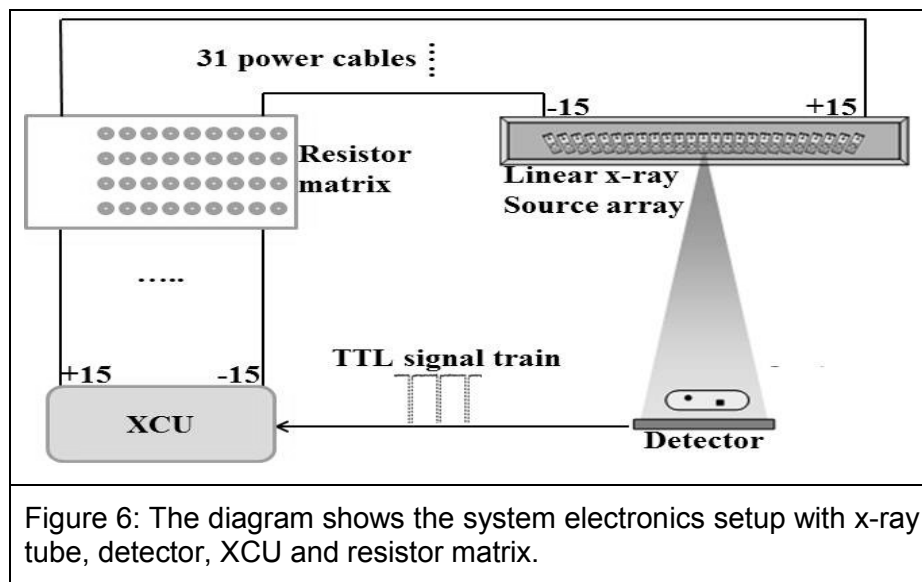
Figure 4 shows the stability of the CNT cathode measured in two different conditions. At 27mA tube current and 250ms pulse width the CNT cathode showed essentially no degradation during the entire 8000 minutes of measurement at 5% duty cycle, which equals to 400 minutes of total x-ray beam-on time, or ~100,000 tomosynthesis scans (15 view and 100mAs per scan) which is estimated to be over 3 years in service lifetime (~60 patients per day, 2 tomosynthesis scan per patient, 250 working days per year). The second test was performed at 38mA and 183ms pulse width. In this case the focal spot size was larger than 0.6mm x 0.6mm. During the ~5000minutes of measurement at 0.6% duty cycle a small increase of the extraction voltage was observed (~8V per 1000 tomosynthesis scans). These two current waveforms were selected for the long term stability test because each pulse provided the dose for one projection view of a 15 view, 100mAs tomosynthesis scan. The present source array is designed to allow ~1000V increase of the extraction voltage without affecting the x-ray output power which means the actual service lifetime could be much longer than this.



c) Detect the generated x-ray radiation and test the electronics circuit;

The stable emission current from the CNT cathode and the cathode to cathode consistency under the anode thermal management allowed current level were also investigated. Figure 5 plots the extraction voltage needed to obtain 27mA tube current from all 31 x-ray sources. The difference between the lowest and the highest extraction voltages is about 400V before any compensation or use of a ballast resistor. The XCU automatically adjusts the gate-cathode voltage to provide the programmed mA value. Figure 5 shows an example of the output current from the central 15 of the 31 x-ray sources. The amplitude of the tube current is controlled by a dedicated XCU which automatically varies the extraction voltage applied to achieve the targeted value which can either be the same for each source or varies in a pre-programmed pattern. Figure 6 shows the system electronics setup.





- d) Measure the x-ray focal spot size following the industrial standard. Any pixel-to-pixel variation in the focal spot size will be corrected by varying the potential of the focusing electrodes

The effective focal spot sizes of the x-ray sources in the array were measured

following the IEC standard using a gold-platinum pin-hole phantom, which is 100 μm in diameter and 500 μm in length and has a 12° opening angle.

The electrical potentials applied to the two focusing

electrodes in the Einzel lens were adjusted to obtain the minimum focal spot size. The same focusing voltages were used for all 31 sources. The measurement was performed at 35kVp anode voltage for all 31 sources.

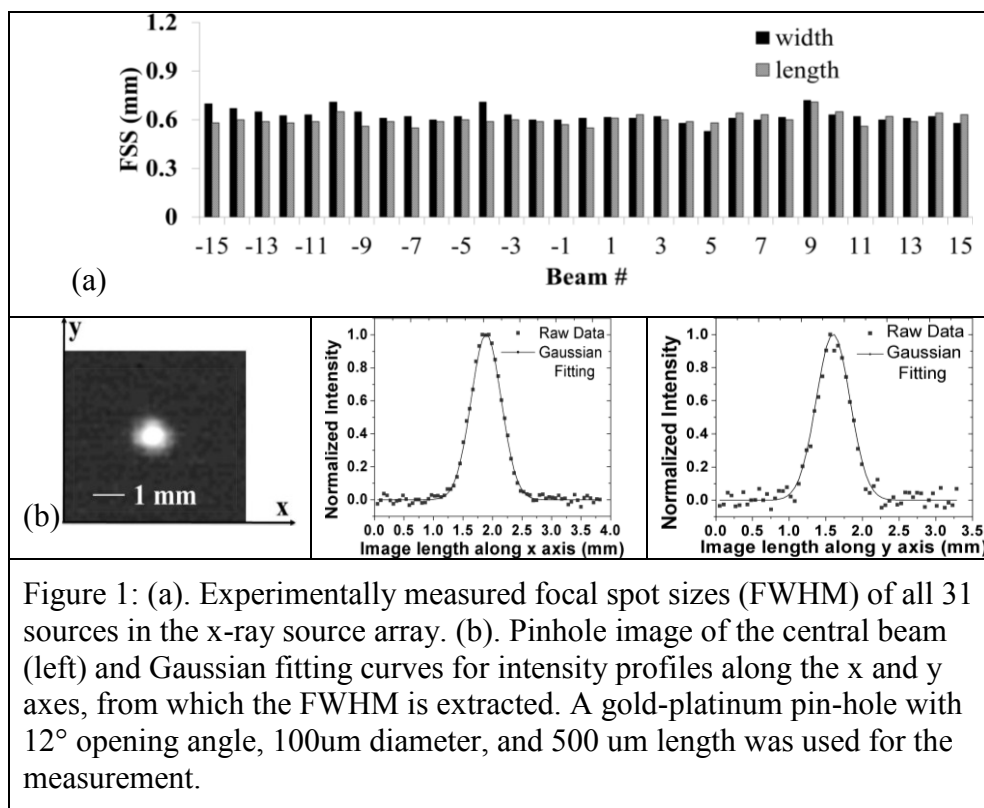


Figure 1 shows the measured focal spot sizes of all 31 x-ray sources of the CNT x-ray source array. Detailed data from the central beam is also shown in Figure 1. The average focal spot size is $0.64 \pm 0.04 \text{ mm} \times 0.61 \pm 0.05 \text{ mm}$ (width x length) at FWHM. The width direction is defined as being parallel to the x-ray source array orientation (scanning direction). The maximum focal spot size in both width and length direction is about 0.7 mm and the smallest dimension is around 0.5 mm.

e) Find the spatial resolution of the system using the modulation transfer function (MTF) phantom

The modulation transfer function (MTF) of the s-DBT scanner was measured using a homemade phantom consisting of a 50 μm diameter W wire. The phantom was mounted on the movable breast compression paddle of the Hologic scanner. The distance between the phantom and the surface of detector can be read from the compression paddle's digital indicator. The wire has a 2° angle with regards to the detector axis, allowing oversampling of the line spread function. The Selenium direct conversion detector was operated in 2x2 binning mode with 140 μm x 140 μm effective pixel size.

Projection images of the MTF wire phantom were acquired using 28 kVp anode voltage, 6.67 mAs dose per view, the 15-view, 14 degree angular coverage mode at a magnification factor of 1.08 (4.4cm thickness). Figure 8 plots the measured MTF from source N7 (#7 source on the left), 0 (central source) and P7 (#7 source on the right) in the s-DBT system. For comparison the corresponding projection MTF's from the rotating gantry system measured at viewing angle of -7, 0 and 7 degrees are also shown on the same figure. The spatial resolutions for the rotating gantry scanner, measured at 10% MTF, are 4 cycles/mm along the scanning direction and 5.4 cycles/mm perpendicular to the scanning direction. These results are consistent with the calculated values using the known system parameters (focus spot size, detector pixel size and SOD). For the s-DBT system, the measured MTF's for the central source (#0) are 5.1 cycles/mm along the scanning direction and 5.2 cycles/mm perpendicular to the scanning direction. The MTF degrades slightly for the off-center x-ray beams. For example, for x-ray beams N7 and P7, the MTF is 5 cycles/mm along the scanning direction. The small variation in MTF for different x-ray beams can be attributed to the projection angle of the x-ray beam on the detector screen. The system MTF obtained using the reconstructed in-focused slice for the two system configurations are plotted in Figure 8. The slice thickness is 1mm. The 10% system MTF is $\sim 1 \text{ cycles/mm}$ lower than the projection MTF for the same system. This is attributed to the reconstruction process and the z-axis offset. When a reconstructed slice does not intersect the object exactly (z-axis offset) the object will be blurred. It has been reported that with 0.5mm z-offset the system MTF can be degraded by as much as 1.5 cycles/mm.

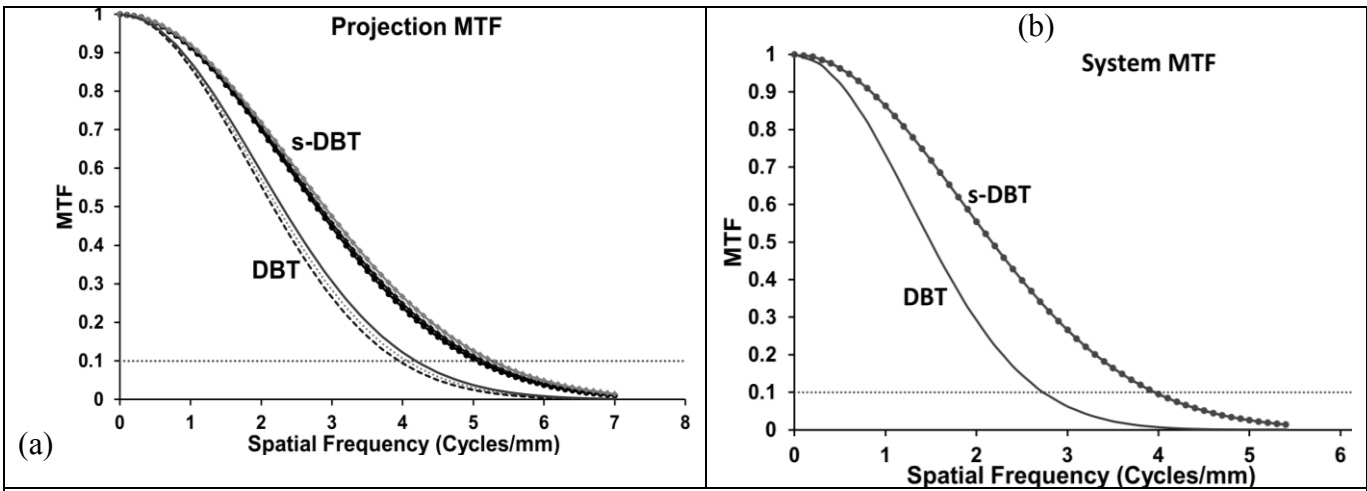


Figure 8. (a). The projection MTF's of the stationary and rotating gantry DBT systems along the scanning direction. (b). The system MTF obtained using reconstructed in-focus slice.

f) Geometry calibration will be performed based on identification of ellipse parameters

The CNT x-ray tube was mounted on the rotating gantry of the Hologic Selenia Dimension scanner replacing its regular rotating anode mammography x-ray tube, as illustrated in Figure 2. A mounting bracket was designed to connect the source array with the gantry and to provide

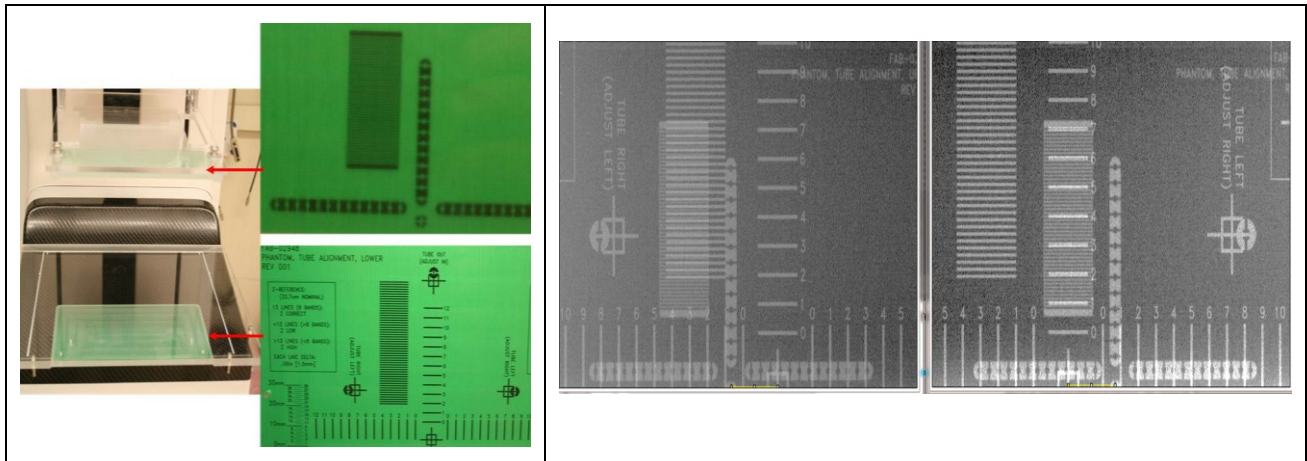


Figure 9. Left: Two geometry alignment phantoms, one is put on the surface of the detector, the other one is mounted on the moving stage which is used to adjust height of the compression paddle. Right: The x-ray source was turned on symmetrically, when the patterns on the top phantom symmetrically aligned with the scales on the bottom phantom the well alignment between the source and the detector was achieved.

multiple degrees of translational and rotational freedom to adjust the exact location of the source with respects to the detector plane. A pair of geometry alignment phantoms were used to align the source and the detector. One phantom was put on the surface of the detector; the other one was mounted on the moving stage which is used to adjust height of the compression paddle, as shown in Figure 9. The x-ray source was turned on symmetrically, when the patterns on the top phantom symmetrically aligned with the scales on the bottom phantom the well

alignment between the source and the detector was achieved. Repeat the procedure with moving stage was at different heights to confirm the well alignment.

A regular geometric calibration was carried out using a tomosynthesis scan of a Hologic Geometric Calibration Phantom. It contains 44 marker balls placed on two planes. Projection matrices were computed for all 31 views using a simple geometry calculation. As a result of geometric calibration, projection matrix was computed for each projection view. It was based on input data including both marker coordinates in 3D object space and projected pixels on the 2D detector. These data usually contain errors due to phantom fabrication, marker position measurement, and 2D projection detection. Calibration sensitivity analysis was carried out by adding uncertainties in input data before projection matrix computation.

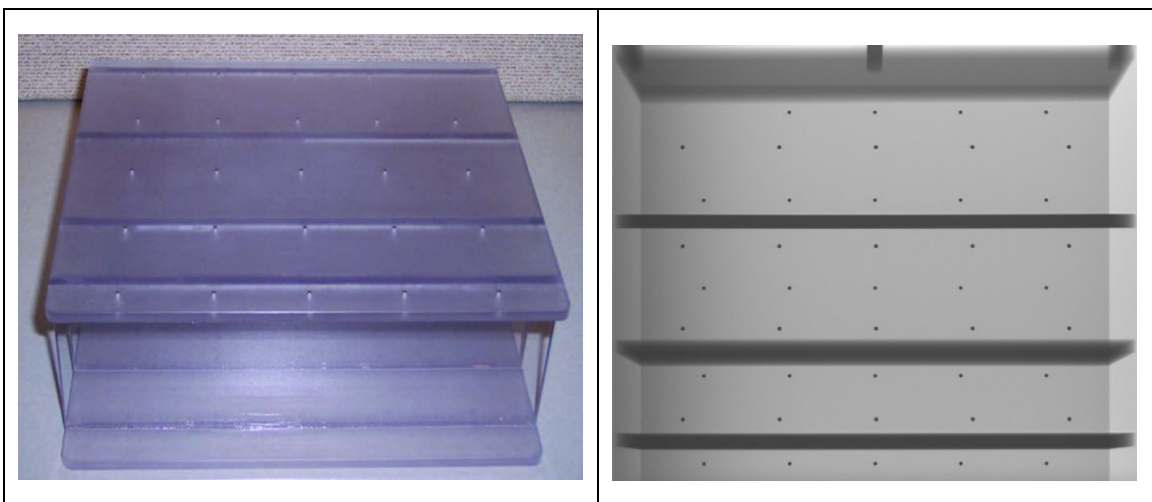


Figure 10. Left: A picture of the Hologic geometric calibration phantom used in this study. Forty four markers are positioned on two planes separated by 76.2 mm. They have a 3D coverage of about 15x15x7.6 cm. Right: X-ray projection image of the phantom using the central beam. From the bottom of the image, markers in rows 1, 3, 5, 7, and 9 are on the bottom plane and markers in rows 2, 4, 6, and 8 are on the top plane.

g) Dose measurements

The quality of tomosynthesis images can depend on many factors such as the angular span of the projection images, the number of projection views, the total dose and dose distribution, the detector resolution and sensitivity, and the reconstruction algorithm. Here we concentrate on dose. The same reconstruction method and detector was used for all imaging configuration.

Four groups of comparison studies were done: (1) For a fixed dose of 100mAs and 15 projection views, we compare the angular span of 14° versus 28° ; (2) For a fixed dose of 100mAs and an angular span of 28° , we compare 15 versus 29 projection views; (3) For a fixed total dose of 100mAs and angular span of 28° and 29 projection views, we compare three different dose distributions; (4) For a fixed angular span of 28° and 29 projection views, we vary

the total dose from 60mAs to 120mAs. All configurations and calculated MTF results are listed in Table 1.

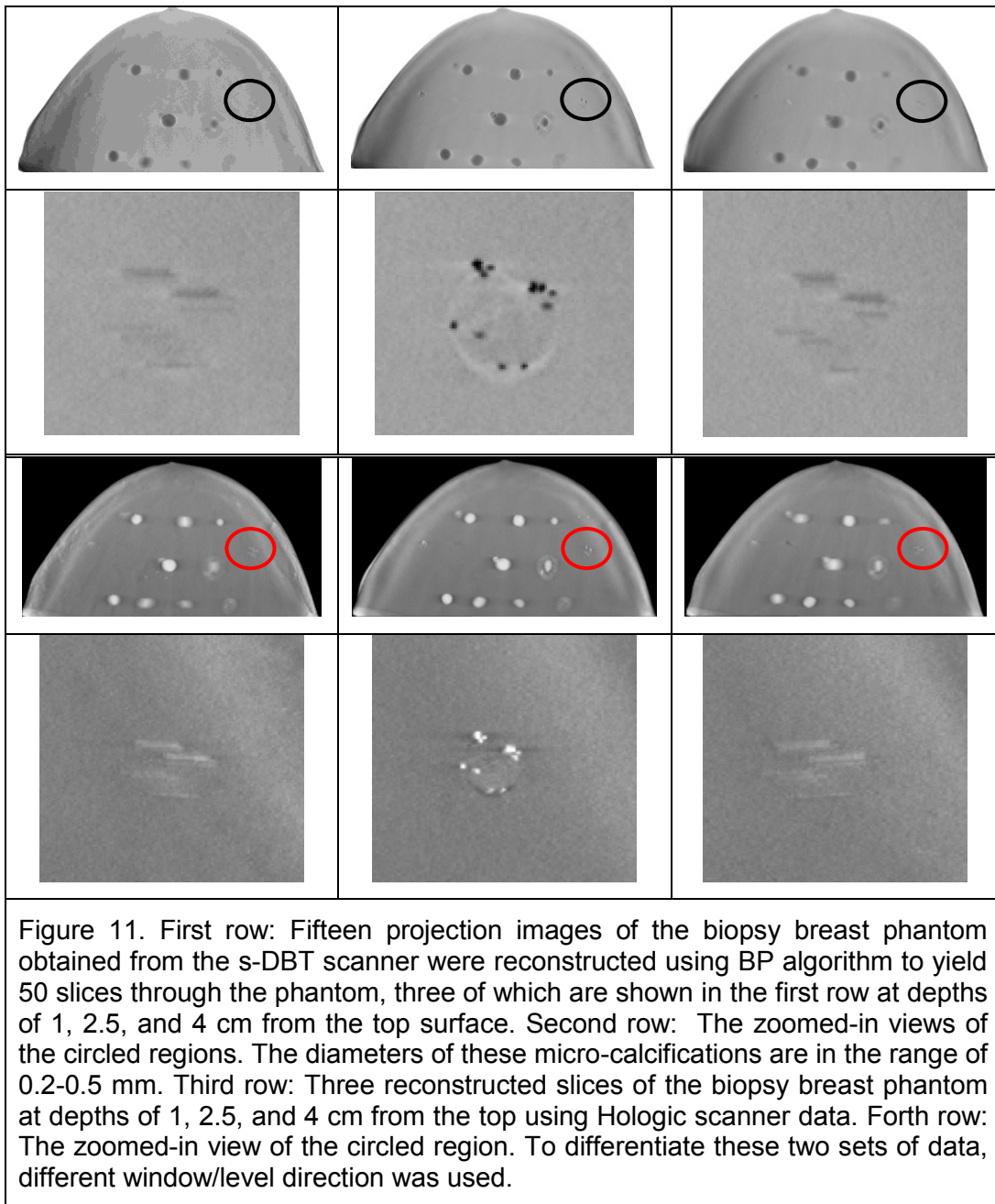
Table 1. Calculated results for MTF using different dose distribution. Data is separated into the four groups of configurations. The configuration with 29 projection views, a 28° angular span, and an even dose distribution resulted in the highest MTF value.					
Group	Number of Projections	Angular Span	Total Dose (mAs)	Dose Distribution	MTF (lps/mm)
1	15	14°	100	Equal dose	4.12
1	15	28°	100	Equal dose	4.13
2	15	28°	100	Equal dose	4.13
2	29	28°	100	Equal dose	4.22
3	29	28°	100	Equal dose	4.22
3	29	28°	100	Lower on central; higher on exterior	4.2
3	29	28°	100	Higher on central; lower on exterior	4.23
4	29	28°	60	Equal dose	4.28
4	29	28°	80	Equal dose	4.25
4	29	28°	100	Equal dose	4.22
4	29	28°	120	Equal dose	4.21

2.2 Characterize the system performance using phantoms: a). Standard breast tissue-equivalent phantom will be used to mimic breast tissues and lesions to evaluate the system performance; b). Reconstructed phantom image quality will be compared with previous published results of commercial DBT prototype scanners. (Months 23-28)

These specific tasks have been achieved.

Projection images of a tissue-equivalent breast phantom (Model 013, CIRS, Inc.) were collected using the s-DBT scanner and the conventional Hologic scanner. The CIRS phantom is shaped to represent a partially compressed breast about 5cm in thickness. Embedded within the CIRS phantom are randomly positioned solid masses and two MC clusters placed in the center layer. The projection images were then reconstructed using the back projection (BP) method and the calculated geometry parameters, yielded 50 slices through the phantom. The slice thickness was 1mm. The images were collected using the following parameters: 15 views over 14 degrees, 28 kVp anode voltage, and a total dose of 100mAs (6.67 mAs per view).

The first row in Figure 11 shows three reconstructed slices of the biopsy breast phantom at depths of 1, 2.5, and 4 cm from the top using s-DBT data. The second row shows the zoomed-in view of the circled region with MC's. The diameters of the micro-calcifications are in the range of 0.2-0.5 mm. The third row shows three reconstructed slices of the biopsy breast phantom at depths of 1, 2.5, and 4 cm from the top using Hologic scanner data. The fourth row shows the zoomed-in view of the circled region with MC's. To differentiate these two sets of data, different window/level direction was used.



2.3 A detailed comparison of the system performance between the new s-DBT scanner and the commercial prototypes will be carried out. (Months 23-28)

These specific tasks have been achieved.

Projection images of the MTF wire phantom were acquired using 28 kVp anode voltage, 6.67 mAs dose per view, the 15-view, 14 degree angular coverage mode at a magnification factor of 1.08 (4.4cm thickness). The measured MTF from source N7 (#7 source on the left), 0 (central source) and P7 (#7 source on the right) in the s-DBT system is plotted in Figure 8. For comparison the corresponding projection MTF's from the Hologic scanner measured at viewing angle of -7, 0 and 7 degrees are also shown on the same figure.

Projection images of an ACR Gammex 156 Mammographic Accreditation phantom were collected using the s-DBT scanner and commercial Hologic scanner. The ACR phantom simulates the x-ray attenuation of a 4.2 cm slab of compressed human breast composed of 50% adipose tissue and 50% glandular tissue. Target objects in ACR phantom are 6 nylon fibrils, 5 simulated micro-calcification specs and 5 masses. All of them are of known size, shape, and density. The projection images were then reconstructed using the back projection (BP) method and the calculated geometry parameters, yielded 50 slices through the phantom. The slice thickness was 1mm. The images were collected using the following parameters: 15 views over 14 degrees, 28 kVp anode voltage, and a total dose of 100mAs (6.67 mAs per view).

The layout of target objects in Gammex 156 ACR phantom is shown in Figure 12. For comparison, the first row (a) and the second row (b) in Figure 12 show a focused slice of the ACR phantom reconstructed using the data collected from the s-DBT and the DBT system, respectively. The three images from left to right in each row are the zoomed-in view of the central MC of the MC Clusters #7, 8, and 9, respectively. The diameters of these 3 MC's are 0.54mm, 0.4mm, and 0.32mm, respectively. The same magnification factor and the window/level are used in displaying the two sets of data. Qualitatively the images in the first row collected using the s-DBT system is clearer.

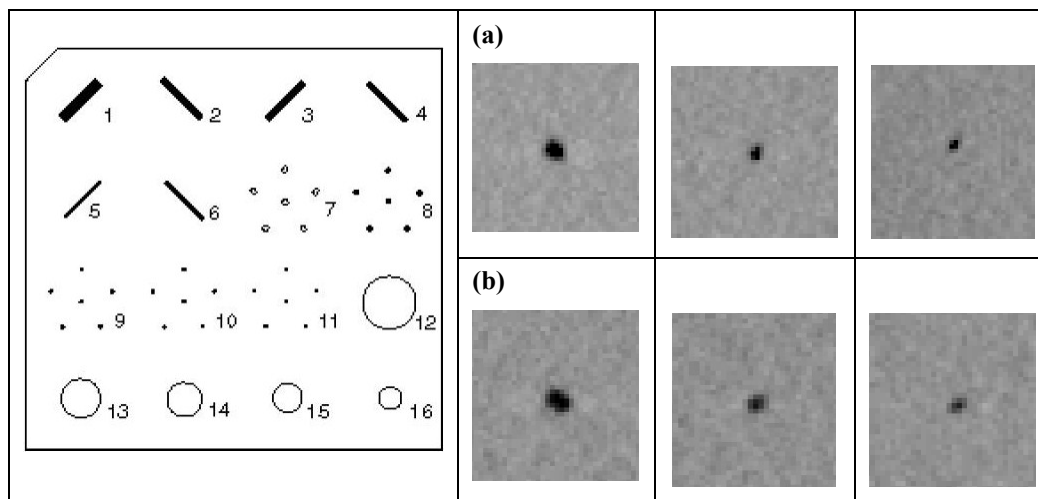


Figure 12. The layout of target objects in Gammex 156 ACR phantom is shown. (a). The first row shows the focused slice of the phantom reconstructed using the s-DBT projection data, (b). The second row shows the focused slice of the phantom reconstructed using the Hologic DBT projection data. The three images from left to right in each row are the zoomed-in view of the central MC of the MC Clusters #7, 8, and 9, respectively. The diameters of these 3 MC's are 0.54mm, 0.4mm, and 0.32mm, respectively. The same magnification factor and the window/level are used in displaying the two sets of data.

Key Research Accomplishments

The motivation of this research project was to improve the spatial resolution and the scanning speed of the current tomosynthesis technology. We successfully constructed an s-DBT system by replacing the regular mammography x-ray tube used in the Hologic Selenia Dimension scanner with a spatially distributed stationary CNT x-ray source array. The s-DBT system is shown to have improved the spatial resolution and the scanning speed compare with DBT tube to complete elimination of the source motion blurring. Although the nominal focal spot size of the mammography x-ray tube used in the DBT scanner is slightly smaller than that of the present CNT x-ray source, the motion blurring is substantial during x-ray exposure which degrades the image quality. In this study using the standard imaging protocol of 15 views over 14 degrees, a 25% improvement in in-plane spatial resolution achieved in the s-DBT design, as shown in Figure 8. The improvement is expected to be more pronounced for a wider angular coverage which is often preferred for better image reconstruction but is difficult to achieve with the rotating gantry design in high speed without significantly degrading the image quality. For the s-DBT scanner, since no mechanical motion is required to collect the multiple projection views, the spatial resolution is independent of the angular coverage. For example the 10% system MTF will remain at ~ 4.0 cycles/mm when the angular coverage is increased from 14 degrees to 30 degrees while all other parameters remain the same for the s-DBT scanner, as shown in Table 2.

To minimize the effect of patient movement on the image quality, it is desired to keep total scanner time as short as possible. The tomosynthesis scanning time T_{scan} of s-DBT is determined by the detector readout time $\Delta t_{readout}$ and the number of projection views N_{view} , but is independent of the angular coverage. It can be expressed as: $T_{scan} = N_{view} \times (\Delta t_{exp} + \Delta t_{readout})$. The exposure time per view Δt_{exp} is set to be the same as the detector integration time, and is a direct function of the total imaging dose (D, in mAs) required, N_{view} , and the x-ray tube current I (in mA) as: $\Delta t_{exp} = D / (N_{view} \times I)$. At 38mA tube current Δt_{exp} is 180ms for a 15-view and 100mAs scan. This translates to a total scan time of 6.3s with current detector readout time of $\Delta t_{readout} = 240ms$, regardless of the angular coverage. On the other hand, the scanning time of DBT depends on the scanning angle. The current Hologic Selenia Dimension scanner takes 3.7s for a 100mAs and 15-view scan at 14 degree coverage. If the angular coverage is increased the same scan will take longer to maintain the same spatial in-plane resolution. The scanning time of the s-DBT can be reduced by increasing the detector speed or/and increasing the x-ray tube current. With advancement of the detector technology flat panel detectors with higher frame rates can potentially be available in the future.

Initial phantom studies demonstrate the capability of the prototype s-DBT system to provide higher quality images, as shown in Figure 12.

Table 2: The spatial resolution and scanning time of the s-DBT system for different imaging protocols		
14°, 15view, 100mAs scan	Scan time	6.3s
	Source motion blur	0
	10% system MTF	4.12 <i>cycles/mm</i>
30°, 15 view, 100mAs scan	Source motion blur	0
	Scan time	6.3s
	10% system MTF	4.13 <i>cycles/mm</i>
30°, 31view, 100mAs scan	Source motion blur	0
	Scan time	10.1s
	10% system MTF	4.2 <i>cycles/mm</i>
Note: The numbers for the 14°, 15 view and 100mAs scan were experimentally measured. The rest was calculated using 28kVp anode voltage, 37mA tube current, 240ms detector readout, 140umx140um detector pixel.		

Reportable Outcomes

Works for year two resulted in some research publications which include:

Journal Articles and Proceedings:

1. **X. Qian**, JP. Lu, O. Zhou, High Resolution Stationary Digital Breast Tomosynthesis Using Distributed Carbon Nanotube X-Ray Source Array, *Medical Physics*, Vol.39, Issue. 4, April 2012
2. **X. Qian**, F. Sprenger, O. Zhou, A Stationary Digital Tomosynthesis Scanner. *ID# 1383-185, SPIE Medical Imaging 2012, San Diego, CA, February 2012*
3. A. Tucker, **X. Qian**, O. Zhou, Optimizing configuration parameters of a stationary digital breast tomosynthesis system based on carbon nanotube X-ray sources, *ID# 1383-6, SPIE Medical Imaging 2012, San Diego, CA, February 2012*

Presentations:

4. **X. Qian**, A. Tucker, O. Zhou, etc.: Stationary Digital Tomosynthesis System for Early Detection of Breast Tumors. *ID# 2676, Era of Hope 2011, Congressionally Directed Medical Research Programs, Orlando, FL, August 2011*
5. **X. Qian**, G. Yang, O. Zhou, A Spatially Distributed X-ray Source Array for High Resolution Digital Tomosynthesis System, *Carolina Center of Cancer Nanotechnology Excellence (CCCNE) and National Cancer Institute (NCI) symposium, June 2011*

Conclusion

Year 2: (May 2011 – April 2012): All aims have been achieved.

- Completion of construction of the MBFEX source and x-ray tube
- Completion of the s-DBT system integration
- Completion of the s-DBT system performance calibration
- The image quality using standard phantom has been characterized using the s-DBT scanner data. The reconstructed images using both s-DBT scanner and Hologic scanner have been compared.
- A detailed comparison of the system performance between the s-DBT scanner and the commercial prototype, Hologic Selenia scanner has been carried out using ACR phantom and MTF phantom.

References

1. Kopans, D.B., *Breast Imaging*. 2nd ed 1997, New York Lippincott Williams and Wilkins
2. Tamara Cherney, P.R., *Breast cancer modality continues decline in Wisconsin*, Wisconsin Medical Journal , . 1999. **98**((4)): p. 47-49.
3. Paci, E., *Mammography and beyond: developing technologies for the early detection of breast cancer*. Breast Cancer Res, 2002. **4**(3): p. 123.
4. Bushberg, J.T., et al., *The essential physics of medical imaging*. Medical Physics, 2003. **30**: p. 1936.
5. Smith, A., et al. *Lesion Visibility in Low Dose Tomosynthesis*. in *International Workshop on Digital Mammography 2006*. 2006. Manchester, UK: Springer-Verlag Berlin Heidelberg 2006.
6. Poplack, S.P., et al., *Digital breast tomosynthesis: initial experience in 98 women with abnormal digital screening mammography*. American Journal of Roentgenology, 2007. **189**(3): p. 616.
7. Niklason, L.T., et al., *Digital tomosynthesis in breast imaging*. Radiology, 1997. **205**(2): p. 399–406.
8. Suryanarayanan, S., et al., *Comparison of tomosynthesis methods used with digital mammography*. Academic radiology, 2000. **7**(12): p. 1085.
9. J.T. Dobbins and D.J. Godfrey, *Digital X-ray tomosynthesis: current state of the art and clinical potential*. Phys. Med. Biol., 2003. **48**: p. 65-106
10. Chen, Y., *Digital breast tomosynthesis (DBT) - a novel imaging technology to improve early breast cancer detection: implementation, comparison and optimization*, 2007, Duke University
11. Anderson, I., *Mammographic screening for breast carcinoma*. Ph.D. thesis, Lund University, Malmo, Sweden, , 1980.
12. Tabar, L., P.B. Dean, and T. Tot, *Radiology of minimal breast cancer*. Radiology, 2000. **217**: p. 54.
13. S. A. Feig, G.S.S., and A. Patchefsky, *Analysis of clinically occult and mammographically occult breast tumors* Am. J. Roentgenol., 1977. **128**,: p. 403-408
14. US-FDA, *Digital Accreditation*, U.D.O.H.H. Services, Editor 2011, <http://www.fda.gov/RadiationEmittingProducts/MammographyQualityStandardsActandProgram/FacilityCertificationandInspection/ucm114148.htm>.
15. Ren, B.R., et al., *A New Generation FFDM/Tomosynthesis Fusion System with Selenium Detector*. Proceeding of SPIE, 2010. **7622**: p. 11.
16. Qian, X., et al., *Design and characterization of a spatially distributed multibeam field emission x-ray source for stationary digital breast tomosynthesis*. Medical Physics, 2009. **36**(10): p. 11.

Appendices

See the following attachments.

High Resolution Stationary Digital Breast Tomosynthesis Using Distributed Carbon Nanotube X-Ray Source Array

Xin Qian¹, Andrew Tucker², Emily Gidcumb³, Jing Shan¹, Guang Yang^{1*}, Xiomara Calderon-Colon^{3*}, Shabana Sultana^{3*}, Jianping Lu^{1,3}, Otto Zhou^{1,3,4}

1. Department of Physics and Astronomy, University of North Carolina at Chapel Hill, Chapel Hill, North Carolina 27599

2. Department of Biomedical Engineering, University of North Carolina at Chapel Hill, Chapel Hill, North Carolina 27599

3. Curriculum in Applied Sciences and Engineering, University of North Carolina at Chapel Hill, Chapel Hill, North Carolina 27599

4. Lineberger Comprehensive Cancer Center, University of North Carolina at Chapel Hill, Chapel Hill, North Carolina 27599

Derrek Spronk, Frank Sprenger

XinRay Systems, Inc., Research Triangle Park, North Carolina 27709

Yiheng Zhang, Don Kennedy, Tom Farbizio, Zhenxue Jing
Hologic Inc, Bedford, MA 01730

Email: xqian@physics.unc.edu; zhou@email.unc.edu

*Current address for Guang Yang: Thermo Fisher Scientific, Minneapolis, MN 55433

*Current address for Xiomara Calderon-Colon: The Johns Hopkins University Applied Physics Laboratory, Laurel, Maryland 20723

*Current address for Shabana Sultana: AMETEK Instruments India Private Limited, Bengaluru, India

Purpose: The purpose of this study is to investigate the feasibility of increasing the system spatial resolution and scanning speed of the current Hologic Selenia Dimensions rotating gantry digital breast tomosynthesis (DBT) scanner by replacing the regular mammography x-ray tube with a specially designed carbon nanotube (CNT) x-ray source array which generates all the projection images needed for tomosynthesis reconstruction by electronically activating individual x-ray sources without any mechanical motion. The stationary digital breast tomosynthesis (s-DBT) design aims to (i) increase the system spatial resolution by eliminating image blurring due to x-ray tube motion and (ii) reduce the scanning time. Low spatial resolution and long scanning time are the two main technical limitations of the current DBT technology.

Methods: A CNT x-ray source array was designed and evaluated against a set of targeted system performance parameters. Simulations were performed to determine the maximum anode heat load at the desired focal spot size and to design the electron focusing optics. Field emission current from CNT cathode was measured for an extended period of time to determine the stable life time of CNT cathode for an expected clinical operation scenario. The source array was manufactured, tested and integrated with a Selenia scanner. An electronic control unit was developed to interface the source array with the detection system and to scan and regulate x-ray beams. The performance of the s-DBT system was evaluated using physical phantoms.

Results: The spatially distributed CNT x-ray source array is comprised of 31 individually addressable x-ray sources covering 30° angular span with 1° pitch and an isotropic focal spot size of 0.6mm at full-width-half-maximum. Stable operation at 28kVp anode voltage and 38mA tube current was demonstrated with extended lifetime and good source-to-source consistency. For the standard imaging protocol of 15 views, 14 degree, 100mAs dose, and 2x2 detector binning the projection resolution along the scanning direction is increased from 4.0 *cycles/mm* (at 10% modulation-transfer-function (MTF)) in DBT to 5.1 *cycles/mm* in s-DBT at magnification factor of 1.08. The improvement is more pronounced for faster scanning speed, wider angular coverage, and smaller detector pixel size. The scanning speed depends on the detector, the number of views, and the imaging dose. With 240ms detector readout time the s-DBT system scanning time is 6.3s for a 15-view, 100mAs scan regardless of the angular coverage. The scanning speed can be reduced to less than 4s when detectors become faster. Initial phantom studies showed good quality reconstructed images.

Conclusions: A prototype s-DBT scanner has been developed and evaluated by retrofitting the Selenia rotating gantry DBT scanner with a spatially distributed CNT x-ray source array. Preliminary results show that it improves system spatial resolution substantially by eliminating image blurring from x-ray focal spot motion. The scanner speed of s-DBT system is independent of angular coverage and can be increased with faster detector without image degradation. The accelerated lifetime measurement demonstrated the long term stability of CNT x-ray source array with typical clinical operation lifetime over 3 years.

Keywords: Breast cancer, digital breast tomosynthesis, carbon nanotube x-ray, s-DBT

1. INTRODUCTION

Breast cancer is the most common type of cancer occurring in women. Early detection is considered as the best hope for decreasing the mortality rate from breast cancer [1-4]. Mammography, the current gold standard for early screening, has played an important role in reducing the mortality rate in the last decade [5, 6]. However, it has well documented limitations including high false positive and false negative rates [7, 8]. Digital breast tomosynthesis (DBT), a limited angle computed tomography technique, has shown significant promises in addressing these limitations [9, 10]. In DBT multiple projection images are acquired at different viewing angles and reconstructed into a 3-D dataset, which can be viewed in thin slices with high in-plane resolution that do not suffer from tissue overlap. It has the potential to improve the effectiveness of early breast cancer screening at a similar dose and comparable cost as the full-field digital mammography (FFDM) [11]. The first commercial DBT scanner received FDA approval in early 2011. Several other DBT systems from different vendors are currently under clinical trials [12-16].

There are however two important limitations of the current DBT technology: low spatial resolution and long scanning time comparing to FFDM. Both result directly from the limitations of the conventional x-ray tube technology where x-ray radiation is generated from a single focal spot and the flux is constrained by the anode heat load. To generate the projection images needed for reconstruction a standard mammography tube is mounted on a rotating gantry and moves along an arc above the partially compressed breast over a certain angular range. The scanning speed and spatial resolution are interconnected and depend on factors including the

total imaging dose, the power of the x-ray tube, the angular coverage, and the number of views [13, 17]. Current DBT systems are grouped into two types. In the step-and-shoot mode (such as GE system) the source needs to come to a complete stop at each position before x-ray exposure. 100 The mechanical instability induced by acceleration and deceleration of the source limits the speed by which the tube can be moved from view to view [18]. In the continuous motion mode (such as Hologic system) the x-ray tube moves continuously through the arc during the scan. The higher the scanning speed, the larger the distance the x-ray tube travels during the finite x-ray exposure time window, and the larger the x-ray focal spot blurring [19, 20]. The amount of focal 105 spot blur that can be tolerated limits the scanning speed and the angular coverage.

Image blurring due to both source and patient motion is a major factor that degrades the spatial resolution of DBT and its sensitivity for small micro-calcifications (MC) compared to FFDM [10]. Although results from phantoms [21, 22] and clinical tests [23] have shown a higher sensitivity for mass compared to mammography, DBT by itself is often inferior to diagnostic 110 mammography in characterization of MC [17], which is critical for diagnosis of cancer [24-26]. The Hologic Selenia Dimension DBT scanner was recently approved by FDA [27] to operate in the combo mode requiring acquisition of both 2D mammography and 3D tomosynthesis images for each patient to achieve good MC and mass detection. This however increases the total imaging dose [12].

To address the limitations of the current DBT technology, we recently demonstrated the 115 concept of stationary digital breast tomosynthesis (s-DBT) in a bench top system using a vacuum chamber based CNT x-ray source array [28]. Instead of mechanically moving a single x-ray tube to the multiple viewing angles, s-DBT employs a stationary x-ray source array which generates x-ray beams from different viewing angles by electronically activating the individual sources 120 (beams) pre-positioned at the corresponding viewing angles without mechanical moving the x-ray tube, therefore eliminating the focal spot motion blurring [29, 30]. The scanning speed is determined only by the x-ray tube flux (which determines the exposure time per view) and the detector readout time, and is independent of angular coverage. Here we report our recent progress in further developing this technology. In particular we investigated the feasibility of 125 improving the spatial resolution of the Hologic Selenia Dimensions DBT scanner by replacing the standard mammography x-ray tube with a specially designed distributed CNT source array. The aim is to increase the detection sensitivity of tomosynthesis for MC's to potentially eliminate the need for additional 2D mammography imaging. We further evaluated the

scanning time at the targeted spatial resolution for a given set of detector readout times. The
lifetime and consistency of the CNT x-ray source array were also tested.

2. METHODS

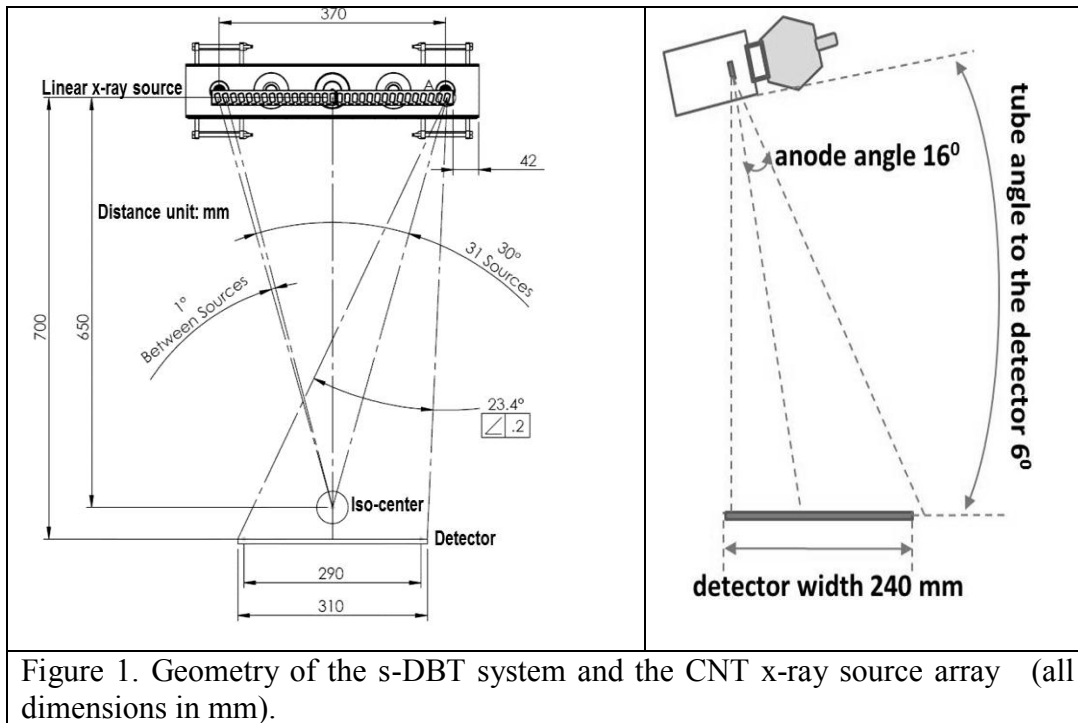
A CNT x-ray source array was designed to have similar imaging configuration to the Selenia Dimensions' except the sources are arranged in a straight line parallel to the detector plane rather than in an arc [12]. Finite element analysis was performed to determine the maximum x-ray tube current at the targeted focal spot size and power. Electron beam optics simulations were carried out to optimize the electron focusing optics to achieve the desired focal spot size. Long term stability and consistency of the CNT cathodes were evaluated. A control electronics system was integrated to scan and regulate the imaging dose from each beam by compensating the driving voltages and by modulating the exposure time from each beam. The x-ray source array was mounted on the gantry of the Selenia Dimensions scanner replacing its original mammography tube and was electronically integrated with the detection unit. Preliminary system calibration was performed using phantoms.

2.1 Overall system configuration and x-ray source design

The CNT source array was designed to provide an imaging configuration similar to the rotating gantry Selenia Dimensions scanner in angular coverage, number of views, and source-detector-distance, as shown in Table 1. It consists of 31 sources distributed in a linear array, inside an evacuated stainless steel housing with a 1mm thick Al window serving as the vacuum barrier and energy filter. The corresponding 31 x-ray focal spots span a distance of 370mm from end to end with equal angular spacing of 1 degree. The x-ray beams can be programmed individually in any time sequence to allow various imaging configurations including 15 views with 14° coverage, 31 views with 30° coverage, and 15 views at 28° coverage at the source-object-distance (SOD) of 650mm. The x-ray anode is tilted 16 degrees and the entire x-ray tube is rotated 6 degrees as illustrated in Figure 1. The x-ray beams are collimated using both internal (inside the tube housing) and external collimators to ensure that x-ray beam from each focal spot covers the whole flat panel detector. The collimation has a tolerance of 2% of the source-imaging-plane distance (SID) on three sides of the detector except the chest wall side, where the beam edge is collimated to within 5mm away from the chest wall [31].

160

Table 1: Specifications of the s-DBT system	
Number of views	Up to 31
Angular range	Up to 30 degrees
Detector FOV	24x29cm
Source-detector distance	700mm
Angular spacing between views	1 degree
X-ray anode	W
Anode tilting angle	16 degrees
Tube rotation	6 degrees
X-ray window	1 mm Al
Anode voltage	Up to 50 kVp
Tube current	Up to 38mA
Focal spot size (FWHM)	0.6mmx0.61mm



Due to manufacturing and cost considerations the 31 x-ray focal spots (sources) in the current design are arranged in a straight line parallel to the detector plane, rather than in an arc with equal distance to the isocenter. In this case the SOD varies slightly from source to source in a simple cosine relation: $SOD_i = SOD_0 / \cos(i * \theta * \pi / 180^\circ)$, where i (the source index) = $0, \pm 1 \dots \pm 15$; θ (the equal angular spacing between the adjacent sources) = 1° ; and $SOD_0 = 650\text{mm}$ is the distance between the central source and the object center (chosen to be the isocenter of the rotating gantry DBT system). To obtain the same entrance dose on the object, the mAs value

170 from each individual source can be adjusted electronically based on its SOD. Each x-ray anode focal spot is individually rotated such that it face toward the center of the object center which is 50mm above the detector surface.

In the present design, the modified Einzel-type electrostatic lens described in our previous publications [28, 33] was utilized. The gate electrode is grounded, the gate-cathode
175 extraction voltage needed to generate the tube current is about 1.4kV. The effective anode kVp is the sum of the anode voltage and the gate-cathode voltage. For example, when anode voltage is set at 28kVp, the effective anode voltage is 29.4kV.

2.2 Anode heat load

180 About 99% of the electron energy of an x-ray tube, whether thermionic or field emission, is wasted as heat on the anode. The maximum operating power is limited by the temperature and heat load of the anode. A mammography x-ray tube typically operates at 100-200mA tube current and ~30kVp effective anode voltage. The peak power of 3-6kW is distributed over the focal track on the rotating anode. In the present CNT x-ray source array design a stationary W
185 anode is used for each focal spot. This allows distribution of the heat load over a larger area. To determine the power limit finite element simulations were carried out using the commercial package (ANSYS). The anode temperature was calculated by solving the heat equation:

$$\rho c_p \frac{\partial T(\vec{x}, t)}{\partial t} = (P_{in} - P_{rad}) \cdot t - \nabla \cdot (k \nabla T(\vec{x}, t))$$

where c_p and k are respectively the temperature dependent heat capacity and thermal
190 conductivity, P_{in} is the input power and P_{rad} is the output power due to blackbody radiation [32].

Thermal simulations were performed on a model structure for various power levels. The power was selected according to the expected operating conditions of the x-ray tube at up to 38kVp effective anode voltage and various tube current and pulse widths. In the current
195 configuration of the CNT tube, the energy of electrons reaching the anode target is the sum of the anode potential and the extraction voltage applied between the gate and the cathode. The maximum simulated effective anode voltage of 38kVp is higher than the most commonly used value for mammography (28kVp) and was chosen to impose more stringent requirement and to take into consideration of imaging conditions for denser and thicker breast. The electron
200 penetration depth into the target is assumed to be constant over the voltage range simulated. The

maximum stable tube current is determined by the heat load of the stationary anode. It depends on the energy, pulse width and the focal spot size. The combinations of 28mA and 250ms, 38mA and 183ms were selected for the anode heat load simulation because each of them provides the necessary dose for a projection view for an imaging protocol of 100mAs per scan with 15 projection views. The temperature distribution on the whole anode structure was simulated for the targeted focal spot size. The power density was distributed on the anode as a Gaussian function with the measured FWHM of the focus spot size [32].

2.3 CNT field emission electron source

Several factors considered in designing the CNT cathode include the targeted focal spot size, the demagnification factor of the electrostatic lens, the anode tilting angle, and the maximum stable emission current density of the CNT emitters. The aim of the present study is to have an isotropic focal spot size of $\sim 0.6\text{mm} \times 0.6\text{mm}$ FWHM which will provide a significant improvement in the spatial resolution along the scanning direction while maintaining a comparable value in the direction orthogonal to motion. The basic structure of each x-ray unit (source) consists of a CNT cathode, a gate electrode to extract electrons, electron focusing lens, and the anode. To focus the field emitted electron beam the modified Einzel-type electrostatic lens described in our previous publications [28, 33] was utilized. The detailed dimension of the electrostatic lens was optimized using a commercial simulation package (OPERA-3D) [34]. The CNT cathodes were fabricated by electrophoretically depositing a composite film comprising pre-formed CNTs and inorganic binders on a metal substrate and by subsequent heat treatment [35].

The emission current from the CNT cathode was evaluated using anticipated operating conditions before the x-ray tube was manufactured with use of a vacuum chamber based test module housing 3 x-ray sources. The test module has a similar structure as the designed tube, with each source consisting of a CNT cathode, an extraction gate, focusing lens, and a W anode. Accelerated lifetime measurements were performed under the pulse mode with variable pulse width and duty cycle. Each pulse corresponds to one x-ray exposure. Long term stability was tested for 250ms and 183ms pulses. During the measurement the extraction electrical field was automatically adjusted to maintain a constant current.

2.4 X-ray focal spot size measurement

235 The effective focal spot sizes of the x-ray sources in the array were measured following the IEC standard [36] using a gold-platinum pin-hole phantom, which is 100 μm in diameter and 500 μm in length and has a 12° opening angle. The electrical potentials applied to the two focusing electrodes in the Einzel lens were adjusted to obtain the minimum focal spot size. The same focusing voltages were used for all 31 sources. The measurement was performed at 35kVp anode voltage for all 31 sources.

240

2.5 System integration

The CNT x-ray source array was mounted on the rotating gantry of the Selenia Dimensions scanner replacing its mammography x-ray tube, as illustrated in Figure 2. A mounting bracket was designed to connect the source array with the gantry and to provide 245 multiple degrees of translational and rotational freedom to adjust the exact location and orientation of the source with respect to the detector plane. The x-ray source array was electronically interfaced with the Selenia detection unit which sets the number of views, the detector integration time, and the detector readout time. The x-ray source exposure time for each view is controlled by the x-ray control unit (XCU). The XCU also controls the current and 250 sequence of the x-ray beams. The pulse width was programmed equal to the detector integration time. A TTL trigger signal from the Selenia detector unit to the XCU synchronizes the x-ray beam activation with the detector integration and readout. The XCU receives a separate trigger pulse from the detector unit for each exposure. During the scan sequence the XCU regulates the extraction voltage for the CNT cathodes to provide the programmed emission current value for 255 each source. The current and the pulse width from each source can be programmed individually to be either the same or various.

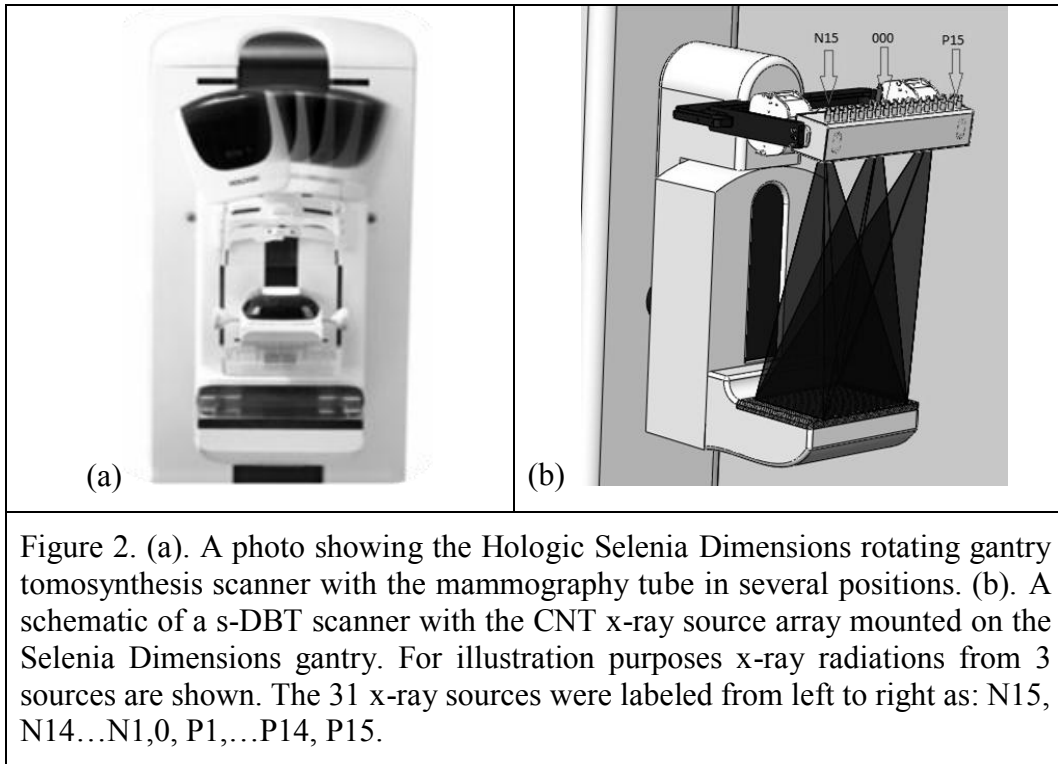


Figure 2. (a). A photo showing the Hologic Selenia Dimensions rotating gantry tomosynthesis scanner with the mammography tube in several positions. (b). A schematic of a s-DBT scanner with the CNT x-ray source array mounted on the Selenia Dimensions gantry. For illustration purposes x-ray radiations from 3 sources are shown. The 31 x-ray sources were labeled from left to right as: N15, N14...N1,0, P1,...P14, P15.

2.6 System calibration

260 The modulation transfer function (MTF) of the s-DBT scanner was measured using a
 homemade phantom consisting of a 50 μm diameter W wire. The phantom was mounted on the
 movable breast compression paddle of the Hologic scanner. The distance between the phantom
 and the surface of detector can be read from the compression paddle's digital indicator. The wire
 has a 2° angle with regards to the detector axis, allowing oversampling of the line spread
 265 function [37]. The Selenium direct conversion detector was operated in 2x2 binning mode with
 140 μm x 140 μm effective pixel size. Images were taken using 28 kVp anode voltage and 6.67
 mAs dose per view.

2.7 Phantom imaging

270 Projection images of a tissue-equivalent breast phantom (Model 013, CIRS, Inc.) and an
 ACR Gammex 156 Mammographic Accreditation phantom were collected using the s-DBT
 scanner and conventional Hologic scanner. The CIRS phantom is shaped to represent a partially
 compressed breast about 5cm in thickness. Embedded within the CIRS phantom are randomly
 positioned solid masses and two MC clusters placed in the center layer. The ACR phantom
 275 simulates the x-ray attenuation of a 4.2 cm slab of compressed human breast composed of 50%

adipose tissue and 50% glandular tissue. Target objects in ACR phantom are 6 nylon fibrils, 5 simulated micro-calcification specs and 5 masses. All of them are of known size, shape, and density. The projection images were then reconstructed using the back projection (BP) method and the calculated geometry parameters, yielded 50 slices through the phantom. The slice thickness was 1mm. The images were collected using the following parameters: 15 views over 14 degrees, 28 kVp anode voltage, and a total dose of 100mAs (6.67 mAs per view).

3. RESULTS

3.1 CNT x-ray source array

Figure 3 shows the CNT x-ray source array designed for s-DBT. The tube contains an extended anode plate with 31 individual tungsten anodes and a two-stage active focusing assembly for electron beam focusing. In the picture one can see the main housing components consist of the HV feed-through for the anode voltage input, two ion getter pumps that allow the monitoring of the pressure inside the tube, and the large x-ray window made from Aluminum. The backside contains the electrical feed-through for the cathodes and the focusing electrodes. The tube was designed to provide similar scan modes as conventional moving source systems. The target material is tungsten in combination with a 1mm Aluminum filtration from the x-ray window. Additional filters and collimators can be installed on the tube housing.

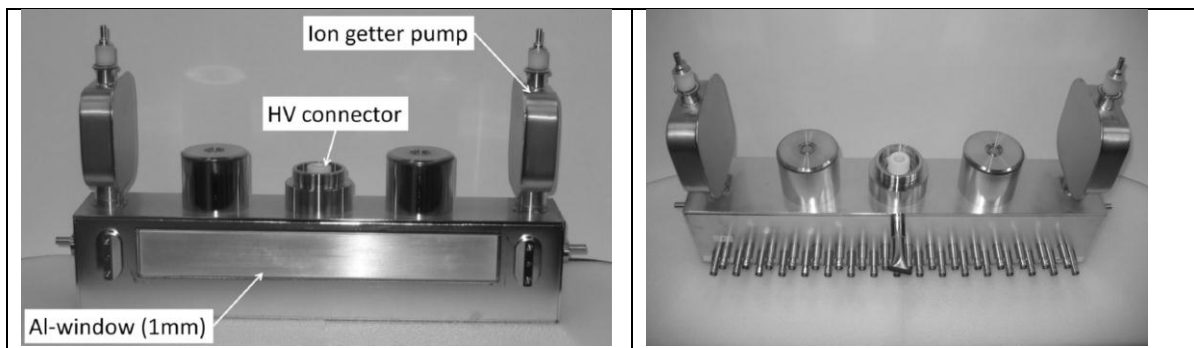
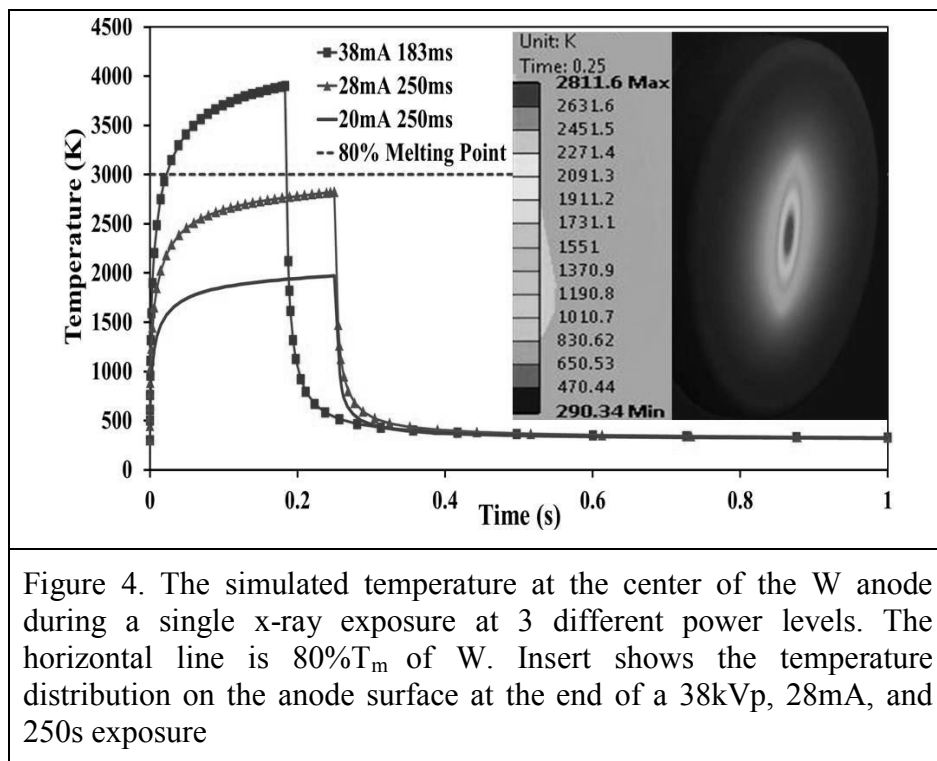


Figure 3. Front and back views of the CNT x-ray source array.

3.2 Anode Heat Load Simulation

Figure 4 shows the simulated anode temperature for exposure conditions listed in Table 2. For the simulation the effective focal spot size was assumed to be 0.6mmx0.6mm FWHM. At 28mA tube current and 250ms pulse width the highest anode temperature was found to be less than 80% of the W melting temperature ($T_m=3695K$), which is generally considered within the

safe operating range. The transient temperature drops very quickly to the base value after the exposure. The anode transient temperature rises with increasing tube power and exceeds the T_m at 38mA and 38kVp. To operate safely at 38mA at this focal spot size the anode voltage needs to be reduced. The temperature becomes substantially lower if 28kVp instead of 38kVp is used in the simulation, which is the most commonly used effective anode voltage for mammography. The anode temperature at 28kVp and 38mA reduces to 2811K, the same as that for the 38kVp and 28mA case. The combinations of 28mA/250ms and 38mA/183ms were selected for the simulation because each provides the necessary dose for a projection view for a tomosynthesis imaging protocol of 100mAs per scan with 15 projection views. The insert is a snap shot of the temperature distribution on the anode surface at the end of a 38kVp, 28mA and 250ms exposure. The temperature drops off quickly from the center of the focal spot.

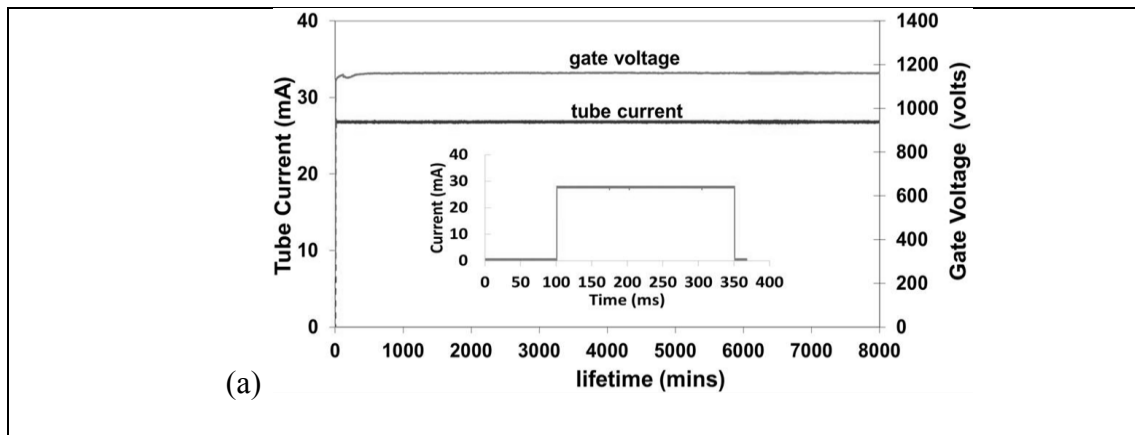


High Voltage (kVp)	Tube Current (mA)	Power (W)	Exposure Time (ms)	Max Temperature (K)
38	38	1444	183	3872
38	28	1064	250	2811
38	20	760	250	1962

315 **3.3 CNT field emission electron source**

The stable emission current from the CNT cathode, the cathode to cathode consistency, and long term stability under the anode thermal management allowed current level were investigated. Figure 5 shows the stability of the CNT cathode measured in two different conditions. At 27mA tube current and 250ms pulse width the CNT cathode showed essentially no degradation during the entire 8000 minutes of measurement at 5% duty cycle, which equals to 400 minutes of total x-ray beam-on time, or ~100,000 tomosynthesis scans. The second test was performed at 38mA and 183ms pulse width. In this case the focal spot size was larger than 0.6mm x 0.6mm. During the ~5000minutes of measurement at 0.6% duty cycle a small increase of the extraction voltage was observed (~8V per 1000 tomosynthesis scans). These two current waveforms were selected for the long term stability test because each pulse provided the dose for one projection view of a 15 view, 100mAs tomosynthesis scan.

It is worth pointing out that as discussed in Section 2.1 the effective anode kVp is the sum of anode voltage and gate-cathode voltage, adjustment of gate-cathode voltage by XCU to maintain the constant current in principle affects the energy of the x-ray spectrum. However, as shown in Figure 5, the adjustment in the gate-cathode voltage over the lifetime test is very small comparing to the anode voltage (<1%). This is because in field emission the current increases exponentially with the applied gate-cathode voltage.



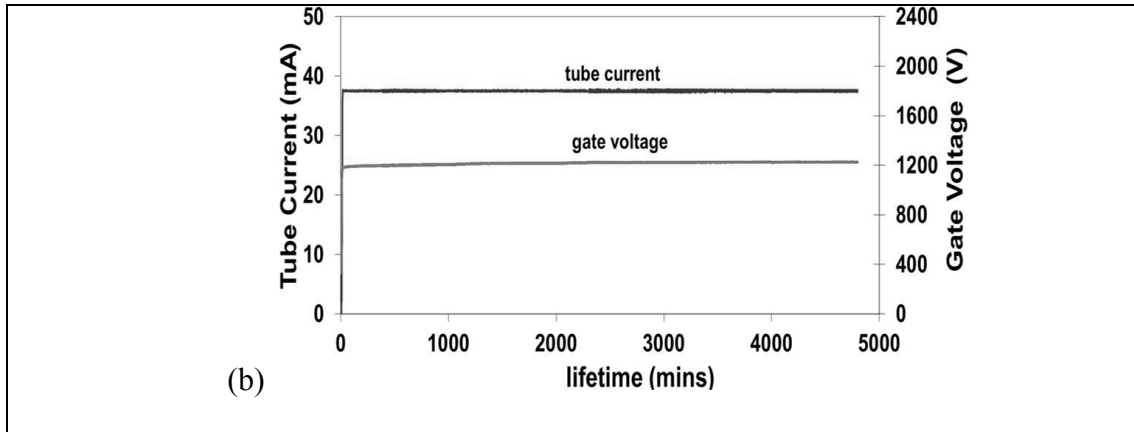


Figure 5: (a). The graph shows lifetime measurement performed at 27mA tube current, 250ms pulse width, and 5% duty cycle. The insert shows one current pulse. (b). The graph shows data at 38mA tube current, 183ms pulse width, 0.6% duty cycle. The extraction voltage was adjusted automatically to maintain constant tube current.

335 The source-to-source consistency of the sealed x-ray tube array was evaluated. Figure 6 plots the extraction voltage needed to obtain 27mA tube current from all 31 x-ray sources. The difference between the lowest and the highest extraction voltages is about 400V before any compensation or use of a ballast resistor. The XCU automatically adjusts the gate-cathode voltage to provide the programmed mA value. Figure 6 shows an example of the output current from the central 15 of the 31 x-ray sources.

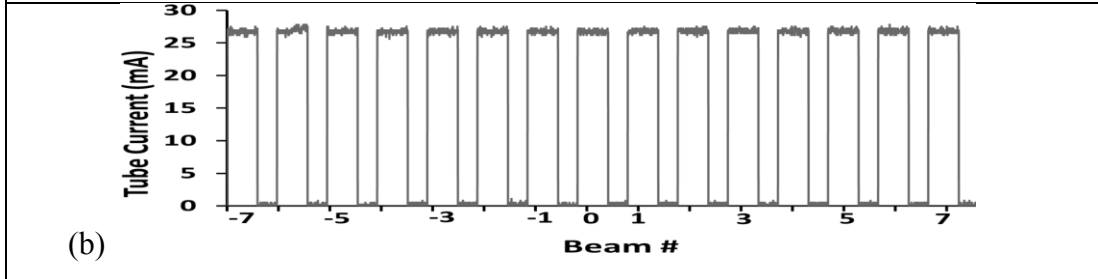
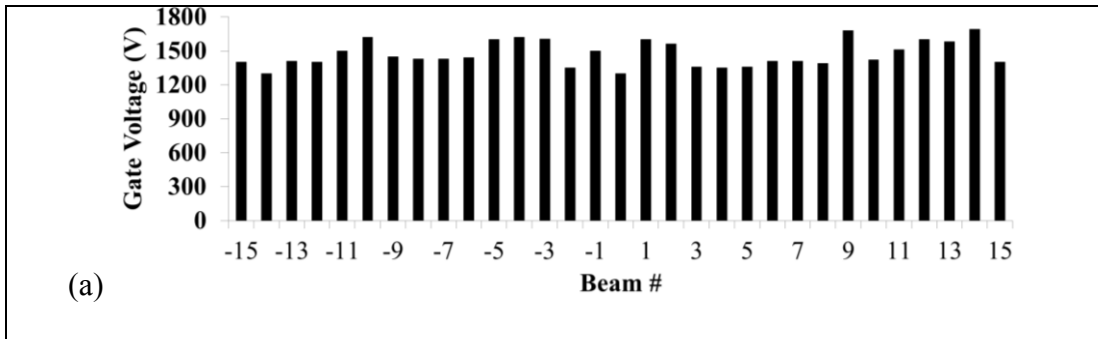


Figure 6: (a). Variation in the extraction voltages needed to obtain 27mA tube current from each CNT cathode in the x-ray source array before any compensation. The average value is about 1.4kV. (b). Tube current from each of the central 15 sources. The XCU automatically adjust the extraction voltage to achieve the required current.

3.4 X-ray focal spot

340 Figure 7 shows the measured focal spot sizes of all 31 x-ray sources of the CNT x-ray source array following the IEC standard [36]. Detailed data from the central beam (source #0) is also shown in Figure 7. The average focal spot size is $0.64 \pm 0.04 \text{ mm} \times 0.61 \pm 0.05 \text{ mm}$ (width x length) at FWHM. The width direction is defined as being parallel to the x-ray source array orientation (scanning direction). The maximum focal spot size in both width and length direction
345 is about 0.7 mm and the smallest dimension is around 0.5 mm.

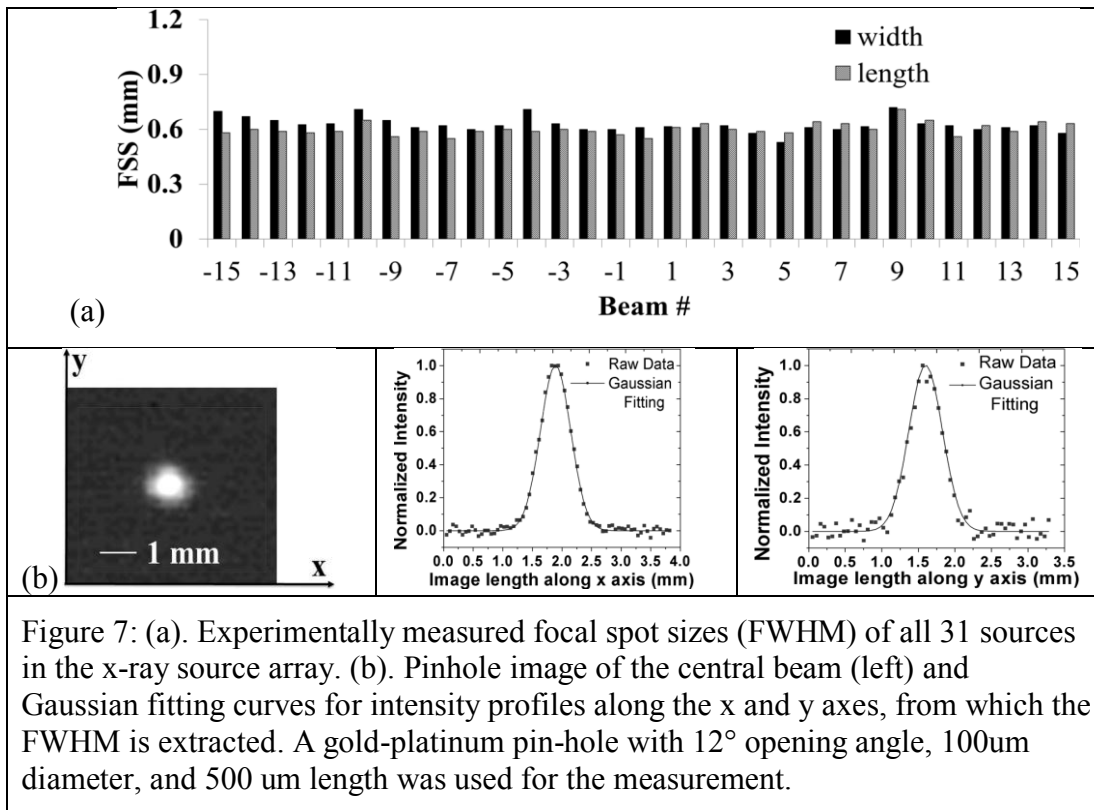
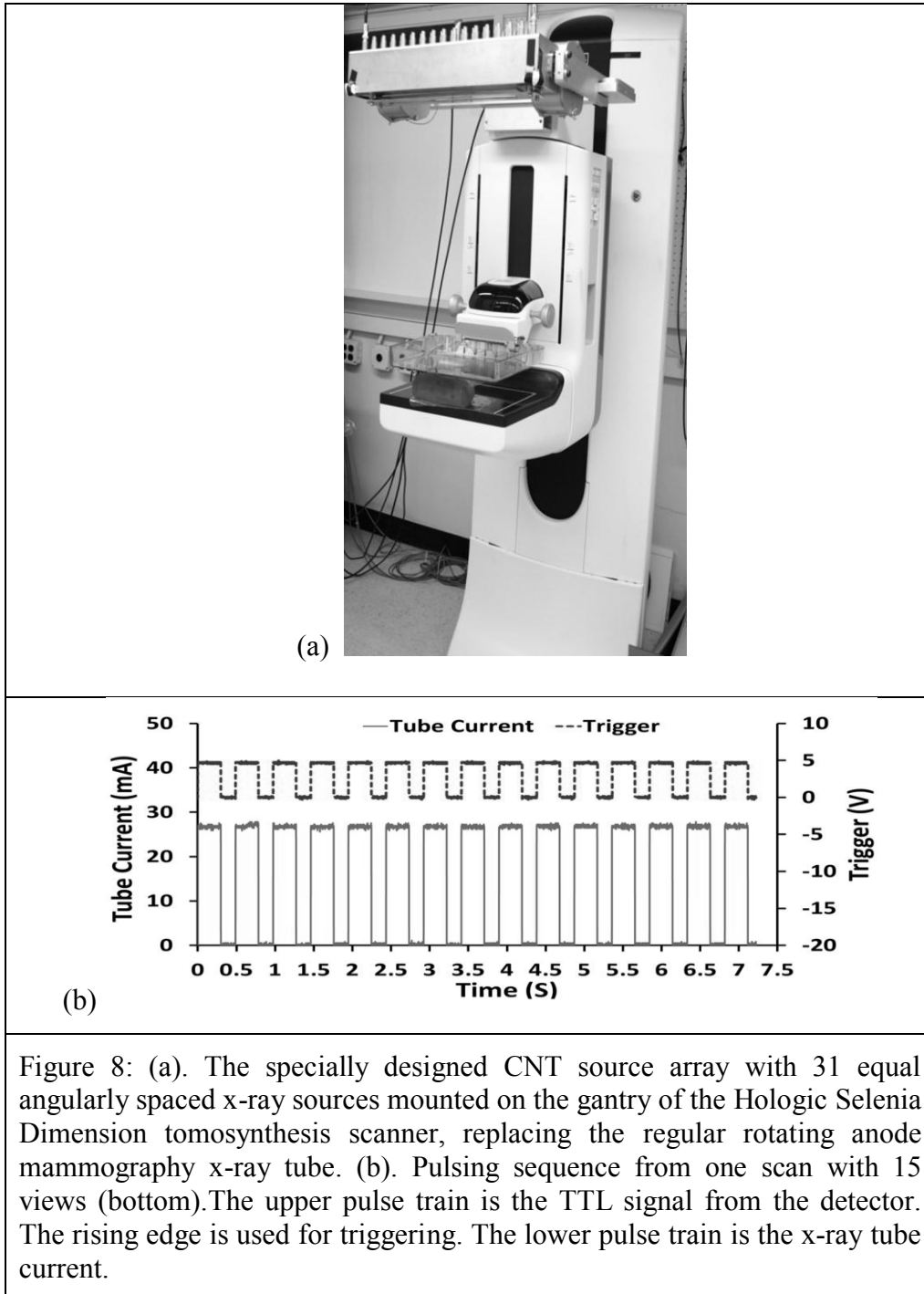


Figure 7: (a). Experimentally measured focal spot sizes (FWHM) of all 31 sources in the x-ray source array. (b). Pinhole image of the central beam (left) and Gaussian fitting curves for intensity profiles along the x and y axes, from which the FWHM is extracted. A gold-platinum pin-hole with 12° opening angle, 100 μm diameter, and 500 μm length was used for the measurement.

3.5 System integration

350 The CNT source array is mounted on the gantry of Hologic Selenia Dimensions tomosynthesis scanner, replacing the regular rotating anode mammography x-ray tube, as shown in Figure 8. Fine adjustment of the position and orientation of the array was made based on the geometry calibration using a phantom containing multiple metal balls. The source is electronically integrated with the detection unit. In the current design exposure from the CNT x-ray source array is driven by the detector. Figure 8 shows an example from one tomosynthesis
355 scan. The detector sent a TTL pulse train signal where each pulse corresponds to one detector frame with pre-set integration and readout time. The rising edge of each pulse triggers exposure

360 from one corresponding x-ray source where the x-ray pulse width is programmed to be the same as the detector integration time. The amplitude of the CNT cathode current, therefore the x-ray tube current, is regulated by the control electronics which automatically varies the extraction voltage applied to achieve the targeted value which can either be the same for each source or varies in a pre-programmed pattern.



3.6 System calibration

Projection images of the MTF wire phantom were acquired using the 15-view, 14 degree
365 angular coverage mode at a magnification factor of 1.08 (4.4cm thickness) and 2x2 detector
binning. Figure 9 plots the measured MTF from source N7 (#7 source on the left), 0 (central
source) and P7 (#7 source on the right) in the s-DBT system. For comparison the corresponding
projection MTF's from the rotating gantry system measured at viewing angle of -7, 0 and 7
degrees are also shown on the same figure. The spatial resolutions for the rotating gantry
370 scanner, measured at 10% MTF, are 4 cycles/mm along the scanning direction and 5.4
cycles/mm perpendicular to the scanning direction. These results are consistent with the
calculated values using the known system parameters (focus spot size, detector pixel size and
SOD). For the s-DBT system, the measured MTF's for the central source (#0) are 5.1 cycles/mm
along the scanning direction and 5.2 cycles/mm perpendicular to the scanning direction. The
375 MTF degrades slightly for the off-center x-ray beams. For example, for x-ray beams N7 and P7,
the MTF is 5 cycles/mm along the scanning direction. The small variation in MTF for different
x-ray beams can be attributed to the projection angle of the x-ray beam on the detector screen
[38]. The system MTF obtained using the reconstructed in-focused slice for the two system
configurations are plotted in Figure 9. The slice thickness is 1mm. The 10% system MTF is
380 ~ 1 cycles/mm lower than the projection MTF for the same system. This is attributed to the
reconstruction process and the z-axis offset. When a reconstructed slice does not intersect the
object exactly (z-axis offset) the object will be blurred. It has been reported that with 0.5mm z-
offset the system MTF can be degraded by as much as 1.5 cycles/mm [19].

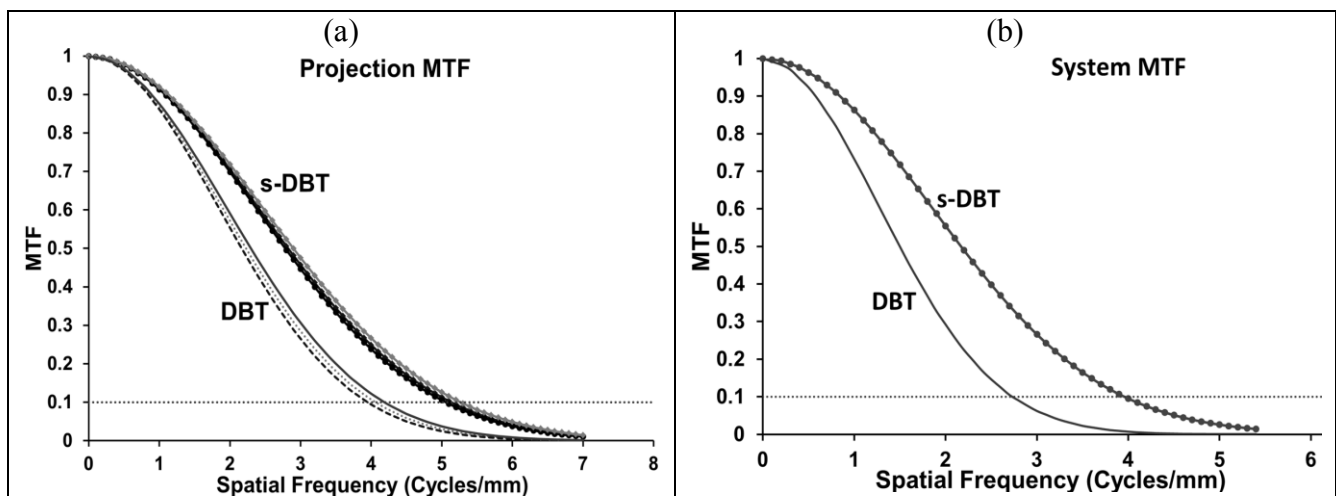


Figure 9. (a). The projection MTF's of the stationary and rotating gantry DBT systems along the scanning direction. (b). The system MTF obtained using reconstructed in-focus slice.

3.7 Initial breast phantom imaging

385 The first row in Figure 10 shows three reconstructed slices of the biopsy breast phantom
at depths of 1, 2.5, and 4 cm from the top. The second row shows the zoomed-in view of the
circled region with MC's. The diameters of the micro-calcifications are in the range of 0.2-0.5
mm. The third row shows three slices of the Gammex 156 ACR phantom at depths of 0.7, 1.4,
and 2 cm from the top. The diameters of these micro-calcifications are 0.54mm. The MCs are
390 most clearly shown in focus at the proper slice location.

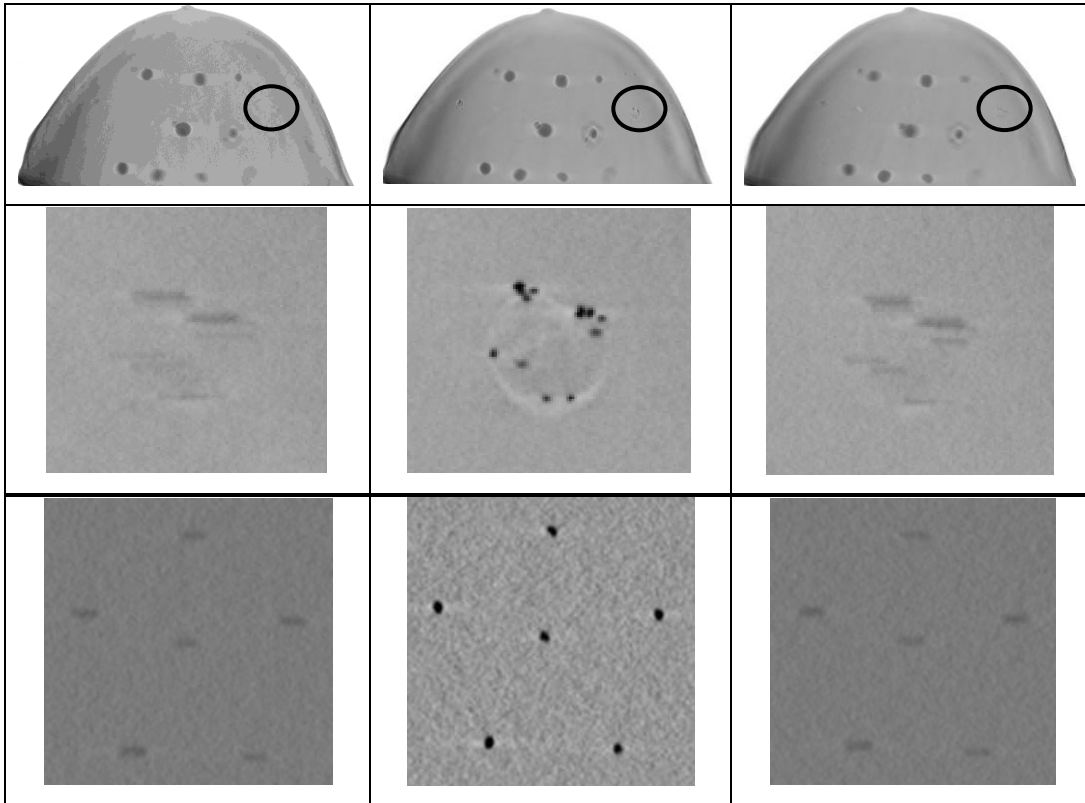
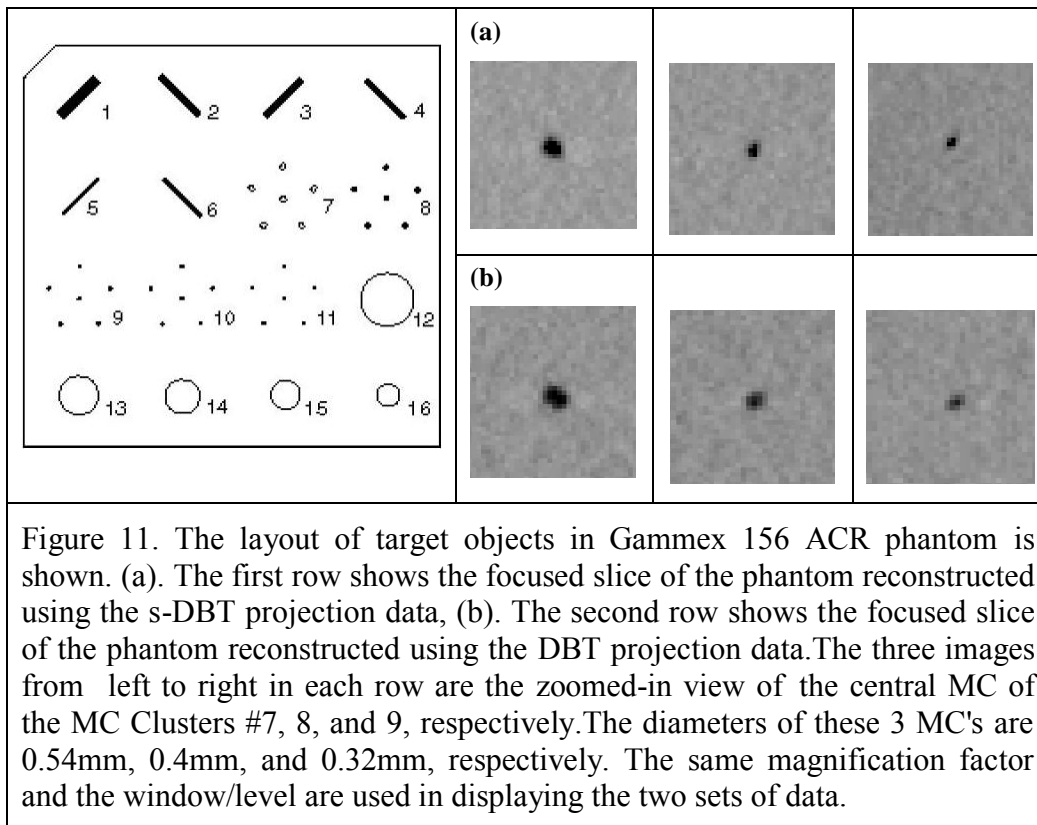


Figure 10. (a). Fifteen projection images of the biopsy breast phantom obtained from the system were reconstructed using BP algorithm to yield 50 slices through the phantom, three of which are shown in the first row at depths of 1, 2.5, and 4 cm from the top surface. (b). The second row shows the zoomed-in views of the circled regions. The diameters of these micro-calcifications are in the range of 0.2-0.5 mm. (c). The third row shows three reconstructed slices of Gammex 156 ACR phantom, which are at depths of 0.7, 1.4, and 2 cm from the top. The diameters of these micro-calcifications are 0.54mm.

The layout of target objects in Gammex 156 ACR phantom is shown in Figure 11. For comparison, the first row (a) and the second row (b) in Figure 11 show a focused slice of the ACR phantom reconstructed using the data collected from the s-DBT and the DBT system, respectively. The three images from left to right in each row are the zoomed-in view of the central MC of the MC Clusters #7, 8, and 9, respectively. The diameters of these 3 MC's are 0.54mm, 0.4mm, and 0.32mm, respectively. The same magnification factor and the window/level are used in displaying the two sets of data. Qualitatively the images in the first row collected using the s-DBT system is clearer.



405

4. Discussion

The motivation of this research project was to improve the spatial resolution and the scanning speed of the current tomosynthesis technology. We successfully constructed a s-DBT system by replacing the regular mammography x-ray tube used in the Hologic Selenia Dimension scanner with a spatially distributed stationary CNT x-ray source array. The s-DBT system is shown to have improved the spatial resolution and the scanning speed compare with DBT tue to complete elimination of the source motion blurring. Although the nominal focal spot size of the

mammography x-ray tube used in the DBT scanner is slightly smaller than that of the present
CNT x-ray source, the motion blurring is substantial during x-ray exposure which degrades the
415 image quality. In this study using the standard imaging protocol of 15 views over 14 degrees, a
25% improvement in in-plane spatial resolution achieved in the s-DBT design. The improvement
is expected to be more pronounced for a wider angular coverage which is often preferred for
better image reconstruction but is difficult to achieve with the rotating gantry design in high
speed without significantly degrading the image quality. For the s-DBT scanner, since no
420 mechanical motion is required to collect the multiple projection views, the spatial resolution is
independent of the angular coverage. For example the 10% system MTF will remain at 4.0
cycles/mm when the angular coverage is increased from 14 degrees to 30 degrees while all other
parameters remain the same for the s-DBT scanner (Table 3).

To minimize the effect of patient movement on the image quality, it is desired to keep total
425 scanner time as short as possible. The tomosynthesis scanning time T_{scan} of s-DBT is
determined by the detector readout time $\Delta t_{readout}$ and the number of projection views N_{view} ,
but is independent of the angular coverage. It can be expressed as: $T_{scan} = N_{view} \times (\Delta t_{exp} +$
 $\Delta t_{readout})$. The exposure time per view Δt_{exp} is set to be the same as the detector integration
time, and is a direct function of the total imaging dose (D, in mAs) required, N_{view} , and the x-ray
430 tube current I (in mA) as: $\Delta t_{exp} = D / (N_{view} \times I)$. At 38mA tube current Δt_{exp} is 180ms
for a 15-view and 100mAs scan. This translates to a total scan time of 6.3s with current detector
readout time of $\Delta t_{readout} = 240ms$, regardless of the angular coverage. On the other hand, the
scanning time of DBT depends on the scanning angle. The current Selenia Dimension scanner
takes 3.7s for a 100mAs and 15-view scan at 14 degree coverage. If the angular coverage is
435 increased the same scan will take longer to maintain the same spatial in-plane resolution. The
scanning time of the s-DBT can be reduced by increasing the detector speed or/and increasing
the x-ray tube current. With advancement of the detector technology flat panel detectors with
higher frame rates can potentially be available in the future.

As a new technology the long term performance of the CNT x-ray source array for
440 tomosynthesis needs to be evaluated. The accelerated lifetime measurement performed under the
condition of 35kVp anode voltage, 27mA tube current, and 0.25s per pulse shows very little
degradation of the CNT cathode during the entire experiment. Here degradation is defined as the
increasing of the extraction voltage for a constant output tube current. The 400mins of total
beam-on time measured from one source, without any noticeable increase of the extraction

445 voltage, is equivalent to 100,000 tomosynthesis scans (15 view and 100mAs per scan) which is
 estimated to be over 3 years in service lifetime (~60 patients per day, 2 tomosynthesis scan per
 patient, 250 working days per year). The present source array is designed to allow ~1000V
 increase of the extraction voltage without affecting the x-ray output power which means the
 450 actual service lifetime could be much longer than this. Initial phantom studies demonstrate the
 capability of the prototype s-DBT system to provide high quality images. Detailed phantom and
 specimen studies are ongoing.

Table 3: The spatial resolution and scanning time of the s-DBT system for different imaging protocols		
14°, 15 view, 100mAs scan	Scan time	6.3s
	Source motion blur	0
	10% system MTF	4.0 <i>cycles/mm</i>
30°, 15 view, 100mAs scan	Source motion blur	0
	Scan time	6.3s
	10% system MTF	4.0 <i>cycles/mm</i>
30°, 31 view, 100mAs scan	Source motion blur	0
	Scan time	10.1s
	10% system MTF	4.0 <i>cycles/mm</i>
Note: The numbers for the 14°, 15 view and 100mAs scan were experimentally measured. The rest was calculated using 28kVp anode voltage, 37mA tube current, 240ms detector readout, 140umx140um detector pixel.		

5. Conclusion

A prototype s-DBT scanner has been developed and evaluated by retrofitting Hologic
 455 Selenia Dimensions rotating gantry DBT scanner with a CNT field emission x-ray source array.
 Preliminary results show that it improves the system spatial resolution by eliminating the image
 blur from x-ray focal spot motion during exposure. The scanning time depends on the detector
 speed and imaging configuration. At small angular coverage the s-DBT scanner is slower but
 becomes comparable and slightly faster than the rotating gantry system at larger coverage angles.
 460 The scanning time can be further reduced without sacrificing the resolution using a faster
 detector. Accelerated lifetime measurement demonstrated the long term stability of the CNT x-
 ray source array for digital breast tomosynthesis.

465

Acknowledgment:

This research was supported by the National Cancer Institute (Grant No. R01CA134598 and U54CA119343) and the University Cancer Research Fund at the University of North Carolina.
470 Dr. X. Qian is supported by a fellowship from the Department of Defense (BC087505). We thank Drs. Y. Chen, G. Cao and YZ Lee for valuable discussions and assistance.

Reference:

1. Kopans, D.B., *Breast Imaging*. 2nd ed 1997, New York Lippincott Williams and Wilkins
475
2. Tamara Cherney, P.R., *Breast cancer mortality continues decline in Wisconsin*, Wisconsin Medical Journal, . 1999. **98**((4)): p. 47-49.
3. Paci, E., *Mammography and beyond: developing technologies for the early detection of breast cancer*. Breast Cancer Res, 2002. **4**(3): p. 123.
- 480 4. Bushberg, J.T., et al., *The essential physics of medical imaging*. Medical Physics, 2003. **30**: p. 1936.
5. Nystrom, L., I. Adnersson, and N. Bjurstam, *Long-term effects of mammography screening: updated overview of the Swedish randomised trials*. Lancet, 2002. **359**(9310): p. 11.
- 485 6. Moss, S.M., H. Cuckle, and A. Evans, *Effect of mammographic screening from age 40 years on breast cancer mortality at 10 years' follow-up: a randomised controlled trial*. Lancet, 2006. **368**(9552): p. 8.
7. Wu, T., et al., *A comparison of reconstruction algorithms for breast tomosynthesis*. Medical Physics, 2004. **31**: p. 2636.
- 490 8. Elmore, J.G., M.B. Barton, and V.M. Moceris, *Ten-year risk of false positive screening mammograms and clinical breast examinations*. N Engl J Med, 1998. **338**(16): p. 7.
9. J.T. Dobbins III and D.J. Godfrey, *Digital x-ray tomosynthesis: current state of the art and clinical potential*. Phys. Med. Biol, 2003. **48**: p. R65-R106.
10. Poplack, S.P., et al., *Digital breast tomosynthesis: initial experience in 98 women with abnormal digital screening mammography*. American Journal of Roentgenology, 2007. **189**(3): p. 616.
- 495 11. Smith, A., et al. *Lesion Visibility in Low Dose Tomosynthesis*. in *International Workshop on Digital Mammography 2006*. 2006. Manchester, UK: Springer-Verlag Berlin Heidelberg 2006.
- 500 12. Ren, B.R., et al., *A New Generation FFDM/Tomosynthesis Fusion System with Selenium Detector*. Proceeding of SPIE, 2010. **7622**: p. 11.
13. M. Bissonnette, et al. *Digital breast tomosynthesis using an amorphous selenium flat panel detector*. in *Medical Imaging 2005: Physics of Medical Imaging, Proceeding of SPIE Vol. 5745*. 2005.
- 505 14. Y. Zhang, et al., *A comparative study of limited-angle cone-beam reconstruction methods for breast tomosynthesis*. Med. Phys., 2006. **33**(10): p. 3781-3795
15. T. Wu, et al., *Tomographic mammography using a limited number of low-dose cone beam projection images*. Med. Phys, 2003. **30**(3): p. 369.
16. A. D. Maidment, et al., *Evaluation of a photon-counting breast tomosynthesis imaging system*. Proc. SPIE, 2006. **6142**: p. 89-99
- 510 17. Chen, Y., *Digital breast tomosynthesis (DBT) - a novel imaging technology to improve early breast cancer detection: implementation, comparison and optimization*, 2007, Duke University

18. Zhou, J., B. Zhao, and W. Zhao, *A computer simulation platform for the optimization of a breast tomosynthesis system*. Medical Physics, 2007. **34**(3): p. 1098-1108.
19. B. Ren, et al., *Design and performance of the prototype full field breast tomosynthesis system with selenium based flat panel detector*. Proc of SPIE, Physics of Medical Imaging, 2005. **5745**.
20. Yorker, J.G., et al. *Characterization of a Full Field Digital Mammography Detector Based on Direct X-ray Conversion in Selenium*. in *Medical Imaging 2002: Physics of Medical Imaging, Proceeding of SPIE*. 2002. San Diego, CA, USA: SPIE.
21. Niklason, L.T., et al., *Digital tomosynthesis in breast imaging*. Radiology, 1997. **205**(2): p. 399–406.
22. Suryanarayanan, S., et al., *Comparison of tomosynthesis methods used with digital mammography*. Academic radiology, 2000. **7**(12): p. 1085.
23. J.T. Dobbins and D.J. Godfrey, *Digital X-ray tomosynthesis: current state of the art and clinical potential*. Phys. Med. Biol., 2003. **48**: p. 65-106
24. Anderson, I., *Mammographic screening for breast carcinoma*. Ph.D. thesis, Lund University, Malmo, Sweden, , 1980.
25. Tabar, L., P.B. Dean, and T. Tot, *Radiology of minimal breast cancer*. Radiology, 2000. **217**: p. 54.
26. S. A. Feig, G.S.S., and A. Patchefsky, *Analysis of clinically occult and mammographically occult breast tumors* Am. J. Roentgenol., 1977. **128**,: p. 403-408
27. US-FDA, *Digital Accreditation*, U.D.O.H.H. Services, Editor 2011, <http://www.fda.gov/RadiationEmittingProducts/MammographyQualityStandardsActandProgram/FacilityCertificationandInspection/ucm114148.htm>.
28. Qian, X., et al., *Design and characterization of a spatially distributed multibeam field emission x-ray source for stationary digital breast tomosynthesis*. Medical Physics, 2009. **36**(10): p. 11.
29. Guang Yang, et al. *Stationary digital breast tomosynthesis system with a multi-beam field emission x-ray source array*. in *SPIE proceeding on Medical Imaging*. 2008.
30. Otto Zhou, et al., *US 7,751,528, Stationary x-ray digital breast tomosynthesis systems and related methods*.
31. FDA, *Radiological Health-Performance Standards for Ionizing Radiation Emitting Products*, in *21*, F.a.D. Administration, Editor 2010.
32. Carslaw, H.S. and J.C. Jaeger, *Conduction of Heat in Solids*1973: Oxford University Press.
33. Zejian Liu, et al., *Carbon nanotube based microfocus field emission x-ray source for microcomputed tomography*. Appl. Phys. Lett., 2006. **89**: p. 103111.
34. J. Zhang, et al., *A nanotube-based field emission x-ray source for micro-computed tomography*. Rev. Sci. Inst. , 2005. **76**: p. 094301.
35. S.J. Oh, et al., *Liquid-phase fabrication of patterned carbon nanotube field emission cathodes*. Appl. Phys. Lett., 2004. **87**(19): p. 3738.
36. IEC, *Medical electrical equipment –X-ray tube assemblies for medical diagnosis*, in *Characteristics of focal spots*2005: Geneva, Switzerland. p. 80.
37. Fujita, e.a., *Simple Method for Determining the Modulation Transfer Function in Digital Radiography*. IEEE Trans Med Imaging, 1992. **11**(1).
38. Badano, A., M. Freed, and Y. Fang, *Oblique incidence effects in direct x-ray detectors: A first-order approximation using a physics-based analytical model*. Medical Physics, 2011. **38**: p. 4.

A Stationary Digital Breast Tomosynthesis Scanner

Xin Qian¹, Andrew Tucker¹, Emily Gidcumb¹, Jianping Lu¹, Otto Zhou¹, Derrek Spronk², Frank Sprenger², Yiheng Zhang³, Don Kennedy³, Tom Farbizio³, Zhenxue Jing³

1 University of North Carolina at Chapel Hill, NC

2 XinRay Systems Inc, Research Triangle Park, NC

3 Hologic Inc, Bedford, MA

ABSTRACT

A prototype stationary digital breast tomosynthesis (s-DBT) system has been developed by retrofitting a Hologic Selenia Dimension rotating gantry tomosynthesis scanner with a spatially distributed carbon nanotube (CNT) x-ray source array. The goal is to improve the system spatial resolution by removing the x-ray tube motion induced focal spot blurring. The CNT x-ray source array comprises 31 individually addressable x-ray beams covering 30° angular span. Each x-ray beam has a minimum focal spot size of 0.64x0.61mm (full-width-at-half-maximum), a stationary W anode operating up to 50kVp, and 1mm thick Al filter. The flux from each beam is regulated and varied using dedicated control electronics. The maximum tube current is determined by the heat load of the stationary anode and depends on the energy, pulse width and the focal spot size used. Stable operation at 28kVp, 27mA tube current, 250msec pulse width and 38mA tube current, 183msec pulse width per exposure was achieved with extended lifetime. The standard ACR phantom was imaged and analyzed to evaluate the image quality. The actual scanning speed depends on the number of views and the readout time of the x-ray detector. With the present detector, 6 second scanning time at either 15 views or 31 views can be achieved at 100mAs total imaging dose with a detector readout time of 240msec.

Keywords: breast cancer, digital breast tomosynthesis, carbon nanotube, field emission

1. INTRODUCTION

Current digital breast tomosynthesis (DBT) scanners require partial isocentric motion of a regular mammography x-ray tube over a certain angular range to record the 2D projection views for reconstructing into a 3D dataset, which can be viewed in thin slices with high in-plane resolution that do not suffer from conventional mammography tissue overlap problem [1, 2]. It has the potential to improve the effectiveness of early breast cancer screening at a similar dose and comparable cost as the full-field digital mammography (FFDM) [3]. The first commercial DBT scanner, Hologic Selenia Dimensions, received FDA approval in early 2011 [4]. Several other DBT systems from different vendors are currently under clinical trials [5-9]. The scanners by Hologic and Siemens operate in a continue motion mode. The x-ray beam is switched on for a short period of time when the tube reaches the viewing position and the detector is in the acquisition window. The motion of the x-ray source during the finite exposure time smears the object and degrades the system resolution. The GE system operates in the step-and-shoot mode where x-ray source comes to a complete stop at each position before x-ray exposure. The system mechanical instability from acceleration and deceleration of the source limits the image quality [10]. The image quality from the current DBT scanners is also compromised by patient motion induced blurring due to the relatively long scanning time [11]. In addition, the already long scanning time prevents further narrowing the x-ray energy bandwidth which has the potential to increase the image contrast but requires a significantly higher x-ray output power in order to maintain a comparable imaging time [12-15].

In this study, we proposed and demonstrated a stationary DBT (s-DBT) prototype scanner by retrofitting a Hologic Selenia Dimension rotating gantry DBT scanner [16] with a CNT distributed x-ray source array [17] which collects the projection views by electronically activating the corresponding x-ray pixels without any mechanical motion. The proposed s-DBT can overcome the addressed limitations of the current DBT scanners. The design and preliminary test result are reported.

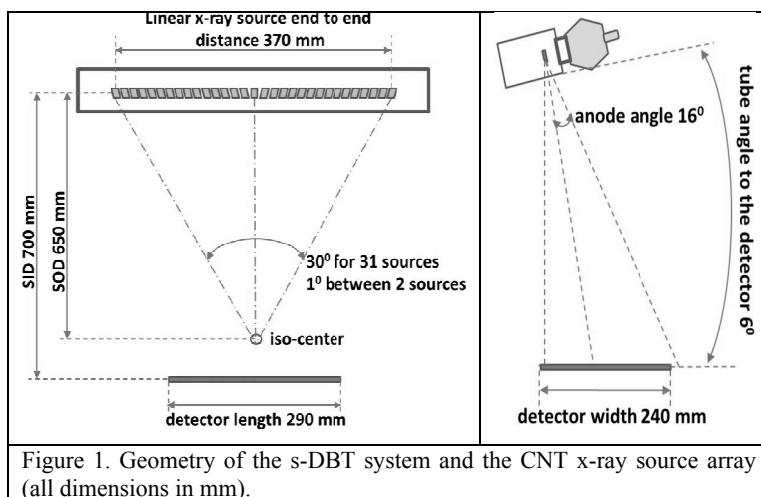
2. METHODS AND MATERIALS

A linear CNT x-ray source array was designed to have a similar imaging configuration as the Hologic Selenia Dimensions scanner except the sources are arranged in a straight line parallel to the detector plane rather than in an arc [5]. Finite element analysis was performed to determine the maximum x-ray tube current at the targeted focal spot size and energy. Electrostatic simulations were carried out to design the electron focusing optics to achieve the desired focal spot size. The emission current from the CNT cathode was evaluated under the anticipated operating conditions before the x-ray tube was manufactured using a vacuum chamber based test module consisting of 3 x-ray sources. The test module has a similar structure as the designed tube, with each source consisting of a CNT cathode, an extraction gate, focusing electrodes, and a W anode. Accelerated lifetime measurements were performed under the pulse mode with variable pulse width and duty cycle. Each pulse corresponds to one x-ray exposure. Long term stability and consistency of the CNT cathodes were evaluated for 250ms and 183ms pulse. The anode voltage was held at 35kVp. A control electronic system was integrated to scan and to regulate the imaging dose from each beam by compensating the driving voltages and by modulating the exposure time from each beam. The finally manufactured x-ray source array was mounted on the gantry of the Hologic Selenia Dimensions scanner replacing its original regular mammography tube and was electronically integrated with the detector. Preliminary system evaluation was performed using standard phantoms.

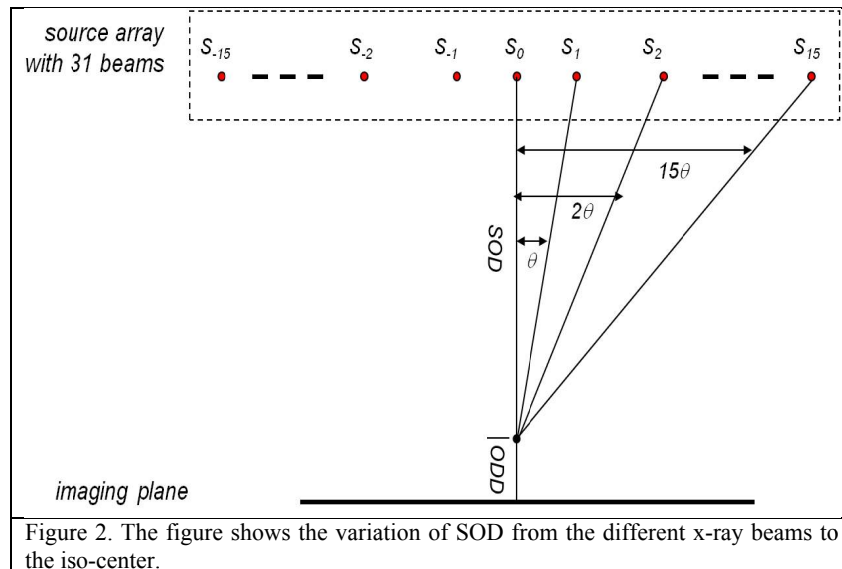
2.1 s-DBT scanner design

The s-DBT system was designed to provide a similar imaging configuration as the rotating gantry Hologic scanner in angular coverage, number of views, source-detector-distance, shown in Table 1. The linear x-ray source array consists of 31 individual beams distributed along a straight line inside an evacuated stainless steel housing with 1mm thick Al window which serves both as the vacuum barrier and the energy filter. The corresponding 31 x-ray focal spots span a distance of 370mm from end to end with equal angular spacing of 1 degree. The x-ray beams can be programmed individually in any time sequence to allow various imaging configurations including 15 views with 14° coverage, 31 views with 30° coverage, and 15 views at 30° coverage at the source-object-distance (SOD) of 650mm. The x-ray anode is tilted by 16 degrees and the entire x-ray tube is rotated by 6 degrees as illustrated in Figure 1. The x-ray beams are collimated using both internal (inside the tube housing) and external collimators to ensure that x-ray beam from each focus spot covers the whole flat panel detector with a tolerance of 2% of the source-imaging-plane distance (SID) on three sides of the detector except the chest wall side, where the beam edge is collimated to within 5mm away from the chest wall [18].

Parameter	Value
Number of views	Up to 31
Angular range	Up to 30 degrees
Detector FOV	24x29cm
Source-detector distance	700mm
Angular spacing between views	1 degree
X-ray anode	W
Anode tilting angle	16 degrees
Tube rotation	6 degrees
X-ray window	1 mm Al
Anode voltage	Up to 50 kVp
Tube current	Up to 38mA
Focal spot size (FWHM)	0.6mmx0.61mm



In the current x-ray source design the 31 x-ray focal spots are arranged in a straight line parallel to the detector plane rather than along an arc. As a result the SOD varies slightly from beam to beam. The central x-ray beam is closer to the object than the beams from the edges, which is in a simple cosine relation: $SOD_i = SOD_0 / \cos(i * \theta * \pi / 180)$, where i (the source index) = $0, \pm 1 \dots \pm 15$; θ (the equal angular spacing between the adjacent sources) = 1° ; and $SOD_0 = 650\text{mm}$. To obtain a constant entrance dose at the object, the mAs value from each beam needs to be regulated according to its respective SOD. This can be accomplished by modulating the corresponding x-ray tube current or x-ray exposure time. Figure 2 shows the variation of the SOD. The x-ray anodes focal spots are rotated towards the center of the object (defined as the iso-center) which is 50mm above the detector surface.



2.2 Linear x-ray source array and electron focusing optics of individual x-ray unit

The appropriate focusing optics has been selected for the proposed x-ray source. This electron optics design is based on computer simulations using a commercial software package (OPERA-3D) to evaluate the modified Einzel lens with three active focusing electrode designs. With less design complications, the goal is to select the design that gives the required focal spot size of $\sim 0.6\text{mm} \times 0.6\text{mm}$ FWHM which will provide sufficient spatial resolution along the scanning direction while maintaining a comparable value in the direction orthogonal to motion. Figure 3 (a) shows the detailed drawings of an individual x-ray beam unit with a modified Einzel lens. The basic structure of each x-ray unit (source) consists of a CNT cathode, a gate electrode to extract electrons, electron focusing lens, and the anode. The gate electrode is grounded, the gate-cathode extraction voltage needed to generate the tube current is about 1.4kV. The

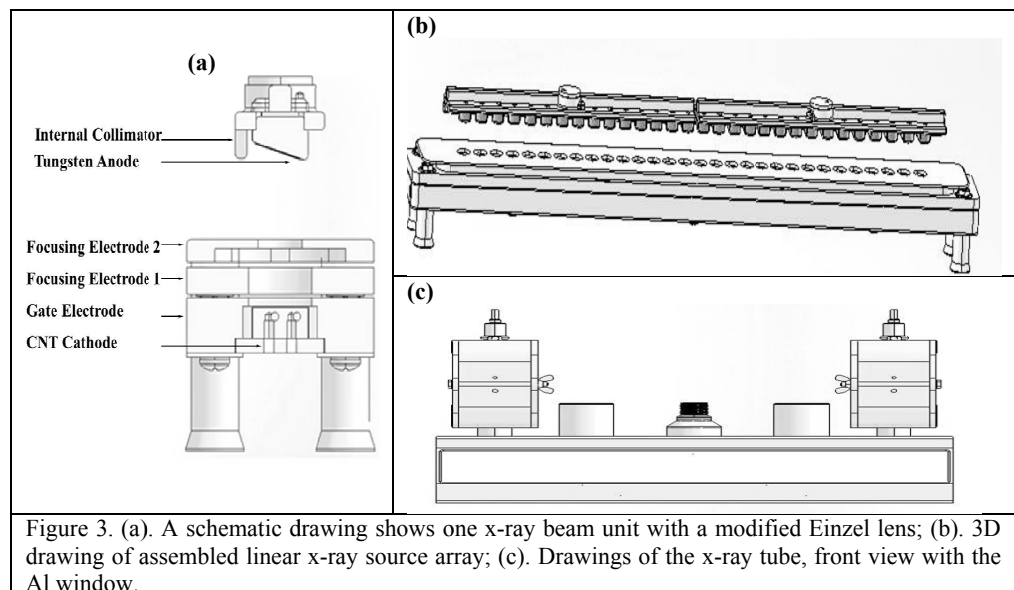


Figure 3 (a) shows the detailed drawings of an individual x-ray beam unit with a modified Einzel lens. The basic structure of each x-ray unit (source) consists of a CNT cathode, a gate electrode to extract electrons, electron focusing lens, and the anode. The gate electrode is grounded, the gate-cathode extraction voltage needed to generate the tube current is about 1.4kV. The

effective anode kVp is the sum of the anode voltage and the gate-cathode voltage. For example, when anode voltage is set at 28kVp, the effective anode voltage is 29.4kV. Figure 3 (b) shows the assembled beam units aligned in a straight line. These assembled beam units will be put into the constructed x-ray chamber. As we can tell from this figure, all the x-ray units have the common gate, focusing electrodes. The anodes are corresponding to individual x-ray units and they are rotated to face the iso-center of the system. Figure 3 (c) shows the front view of the x-ray tube.

2.3 Anode heat load

The main source of thermal energy generation in a field emission x-ray tube, as well as a thermionic x-ray tube, results from bombardment of the high kinetic energy electrons on the metal anode. About 99% of the kinetic energy of the electron is converted to heat on the anode. A conventional rotating anode mammography x-ray tube operates at 100-200mA tube current at ~30kVp effective anode voltage, resulting in a peak power of 3-6kW. The rotating anode design is used to distribute the thermal load over a large area. In the case of the linear x-ray source array designed for the proposed s-DBT scanner, the anode is an extended metallic structure. The thermal energy is distributed over the full length and the anode block has sufficient heat capacity to absorb the thermal energy generated during the scan. The energy input of 100mAs x 40kV = 4kJ leads to a very small temperature rise compared with temperature rise in conventional x-ray tubes. The peak power of the MBFEX source is only ~1kW. This power has to be removed from the tube to allow a scan every 30s. However there is a concern whether the individual focus spot will be heated up too close to the melting temperature of the target material for the time duration the electron beam is on. To determine the power limit finite element simulations were carried out using a commercial package (ANSYS). The anode temperature was calculated by solving the heat equation:

$$\rho c_p \frac{\partial T(\vec{x}, t)}{\partial t} = (P_{in} - P_{rad}) \cdot t - \nabla \cdot (k \nabla T(\vec{x}, t))$$

where c_p and k are respectively the temperature dependent heat capacity and thermal conductivity, P_{in} is the input power and P_{rad} is the output power due to blackbody radiation [19]. Thermal simulations were performed on a model structure for various power levels. The power was selected according to the expected operating conditions of the x-ray tube at up to 38kVp effective anode voltage and various tube current and pulse widths. The electron penetration depth into the target is assumed to be constant over the effective anode voltage range of 28 to 38kVp. The temperature distribution on the whole anode structure was simulated for the targeted focal spot size.

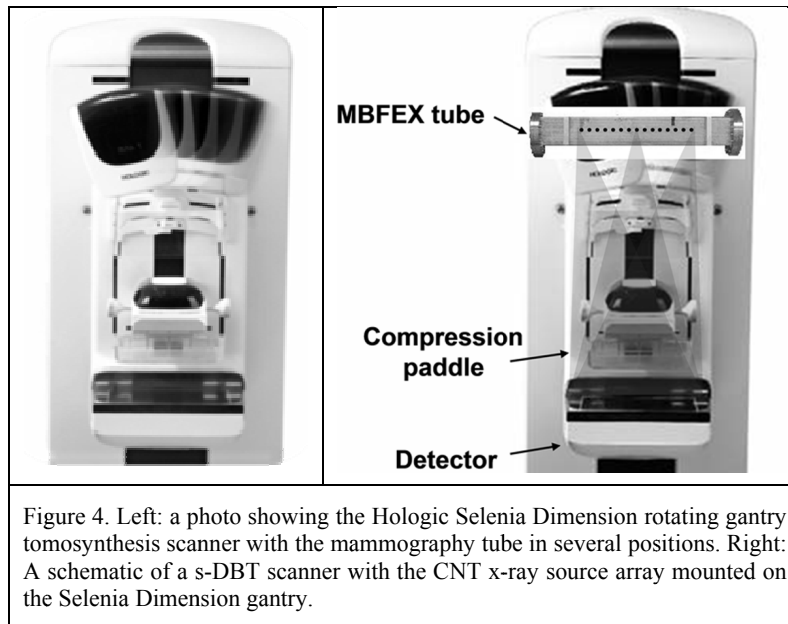
2.4 X-ray focal spot size measurement

The effective FSS of the x-ray beam has been measured using a gold-platinum pin-hole phantom. The diameter of the pinhole is $d=100\mu\text{m}$ with 500 μm length and 12° opening angle. The FSS was measured regarding the IEC standard [20]. Each x-ray generating unit comprises a CNT field emission cathode, a gate electrode to extract the electrons, and two modified Einzel-type electrostatic lenses to focus the field emitted electrons to a small area on a Tungsten anode. The anode, focusing electrodes and the cathode will be electrically connected to the following 4 power supplies respectively: Spellman SR70PN6 (70KV, 85mA), Stanford Research PS350 (2.5KV, 10mA), and Keithley 248 (5KV, 5mA), Glassman ER03R100 (3KV, 100mA). The electrical potentials applied to the two focusing electrodes in the Einzel lens were adjusted to obtain the minimum focal spot size. The same focusing voltages were used for all 31 sources. The measurement was performed at 35kVp anode voltage for all 31 sources.

2.5 System integration

The CNT x-ray source array was mounted on the rotating gantry of the Selenia Dimension scanner replacing its mammography x-ray tube, as illustrated in Figure 4. A mounting bracket was designed to connect the source array with the gantry and to provide multiple degrees of translational and rotational freedom to adjust the exact location and orientation of the source with respects to the detector plane. The x-ray source array was electronically interfaced with the Selenia detection unit which sets the number of views and the detector integration and readout times. The x-ray source exposure time for each view is controlled by the x-ray control unit (XCU). The XCU also controls the current and sequence of the x-ray beams. The pulse width was programmed to be the same as the detector integration time. A TTL trigger signal from the Selenia detector unit to the XCU synchronizes the x-ray beam activation with the detector integration and readout. The XCU receives a separate trigger pulse from the detector unit for each exposure. During the scan sequence the XCU regulates the extraction voltage for the CNT cathodes to provide the programmed emission

current value for each source. The current and the pulse width from each source can be programmed individually to be either the same or various.



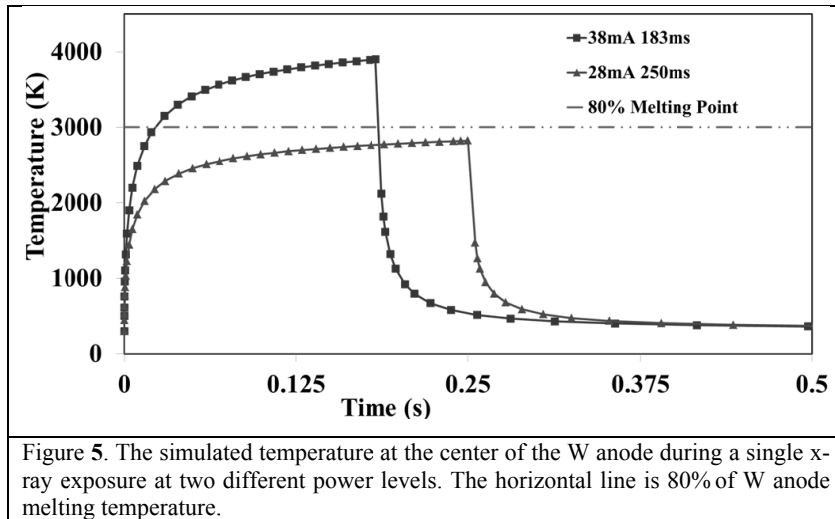
2.6 Initial phantom imaging

Projection images of an ACR Gammex 156 Mammographic Accreditation phantom were collected using both the s-DBT scanner and original Hologic Dimensions scanner. The ACR phantom simulates the x-ray attenuation of a 4.2 cm slab of compressed human breast composed of 50% adipose tissue and 50% glandular tissue. Target objects in this phantom are composed of nylon fibrils, simulated micro-calcification specs and masses. All of them are of known size, shape, and density. The projection images were then reconstructed using the back projection (BP) method and the calculated geometry parameters to yield 50 slices through the phantom. The slice thickness was 1mm. The images were collected using the following parameters: 15 views over 14 degrees, 28 kVp, and 100 mAs.

3. RESULTS

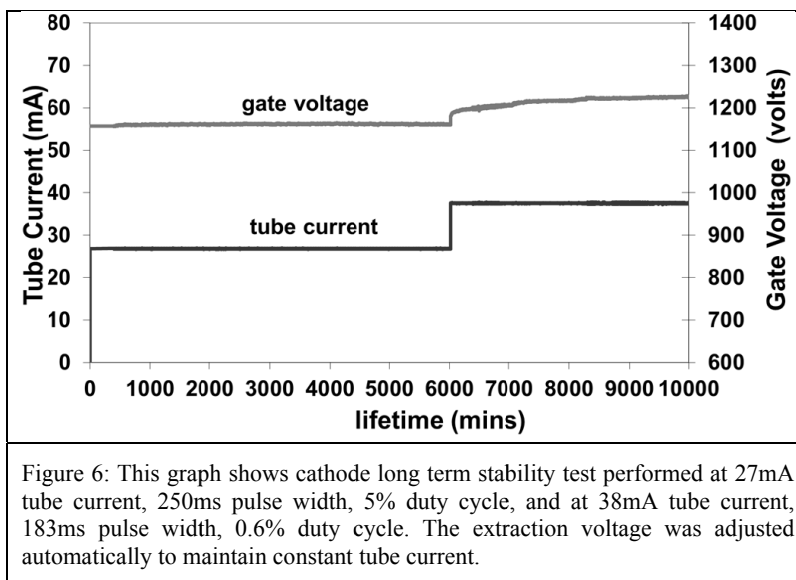
3.1 Anode Heat Load Simulation

Figure 5 shows the simulated anode temperature for two different exposure conditions, 38mA tube current and 183ms pulse width, and 28mA tube current and 250ms pulse width. The combinations of 28mA/250ms and 38mA/183ms were selected for the simulation because each provides the necessary dose for a projection view for a tomosynthesis imaging protocol of 100mAs per scan with 15 projection views. Effective anode voltage, 38kVp, higher than the most commonly used value for mammography (28kVp) was chosen to impose more stringent requirement and to take into imaging consideration for denser and thicker breast. For the simulation the effective focal spot size was assumed to be 0.6mmx0.6mm FWHM. At 28mA tube current and 250ms pulse width the highest anode temperature was found to be less than 80% of the W melting temperature (3695K), which is generally considered as within the safe operating range. The transient temperature drops very quickly to the base value after the exposure. The anode transient temperature rises with increasing tube power and exceeds the anode melting temperature at 38mA and 38kVp. To operate safely at 38mA at this focal spot size the effective anode voltage needs to be reduced to 28KVp. The anode temperature at 28kVp and 38mA reduces to 2811K, the same as that for the 38kVp and 28mA case.

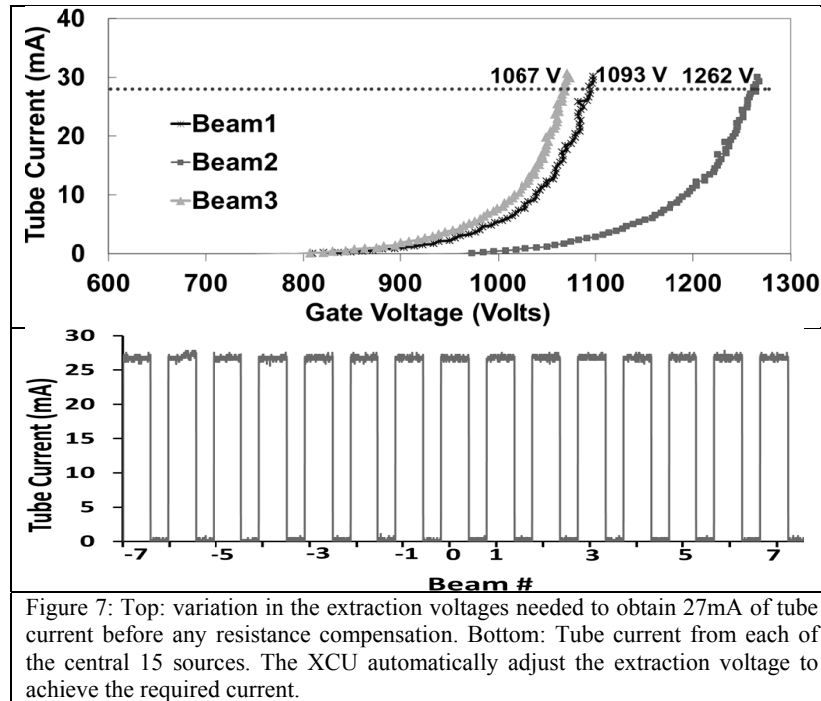


3.2 CNT field emission electron source

Figure 6 shows the cathode long term stability measurement results. The experiment was performed in two different conditions: 27mA tube current, 250ms pulse width, and 5% duty cycle, and data at 38mA tube current, 183ms pulse width, 0.6% duty cycle. As we can see, at 27mA tube current and 250ms pulse width the cathode shows no degradation after 8000 minutes measurement time, the total x-ray on time is 424 minutes. Since the x-ray on time per scan per beam is 250ms, the cathode can last from ~ 100,000 scans. For a busy mammography clinic with ~ 60 patients per day, 2 scans per patients, 200 working days per year. The results mean that CNT source can last for at least 4 years. The second test was performed at 38mA and 183ms pulse width. During the ~4000minutes of measurement at 0.6% duty cycle a small increase of the extraction voltage was observed (~8V per 1000 tomosynthesis scans). These two current waveforms were selected for the long term stability test because each pulse provided the dose for one projection view for a 15 view and 100mAs tomosynthesis scan. The higher the tube current is, the shorter the total scan time is.

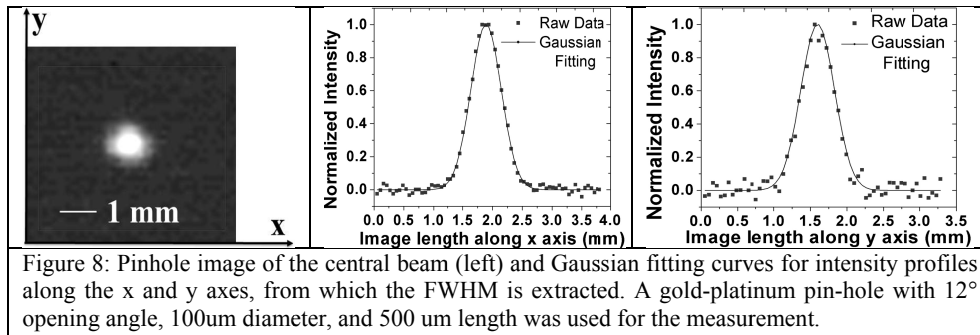


The source-to-source consistency of the sealed x-ray tube array was evaluated. Figure 7 plots the extraction voltage needed to obtain 27mA tube current. The difference between the lowest and the highest voltages is about 200V before any compensation using ballast resistors. The XCU automatically adjusts the gate-cathode voltage to provide the programmed mA value. Figure 7 shows an example of the output current from the central 15 of the 31 x-ray sources.



3.4 X-ray focal spot

Focal spot sizes of all 31 x-ray beams of the CNT x-ray source array were measured following the IEC standard [20]. Detailed data from the central beam (source #0) is shown in Figure 8. The average focal spot size for all 31 beams is $0.64 \pm 0.04 \text{ mm} \times 0.61 \pm 0.05 \text{ mm}$ (width x length) at FWHM. The width direction is defined as being parallel to the x-ray source array orientation (scanning direction). The maximum focus spot size in both the width and length direction is about 0.7 mm and the smallest dimension is around 0.5 mm.



3.5 System integration

The specially designed linear source array with 31 equal angularly spaced x-ray beams is mounted on the gantry of the Hologic Selenia Dimension tomosynthesis scanner, replacing the regular mammography x-ray tube, as shown in Figure 9. In order to determine the location of each individual x-ray source and adjust the overall position of CNT x-ray source array, geometry calibration was performed using a phantom containing multiple metal balls. The source is electronically integrated with the detector. In the current design exposure from the CNT x-ray source array is driven by the detector. A TTL signal train is sent from the detector to the XCU. XCU then turns on x-ray units in programmed sequence. A resistor matrix linked between XCU and x-ray tube is used to compensate gate voltage to provide preset tube current. **Error! Reference source not found.** Figure 9 shows an example from one tomosynthesis scan. The detector sent a TTL pulse train signal where each pulse corresponds to one detector frame with pre-set detector integration and readout time. The

rising edge of each pulse triggers exposure from one corresponding x-ray source where the x-ray pulse width is programmed to be the same as the detector integration time. The amplitude of the tube current is controlled by a dedicated XCU which automatically varies the extraction voltage applied to achieve the targeted value which can either be the same for each source or varies in a pre-programmed pattern.

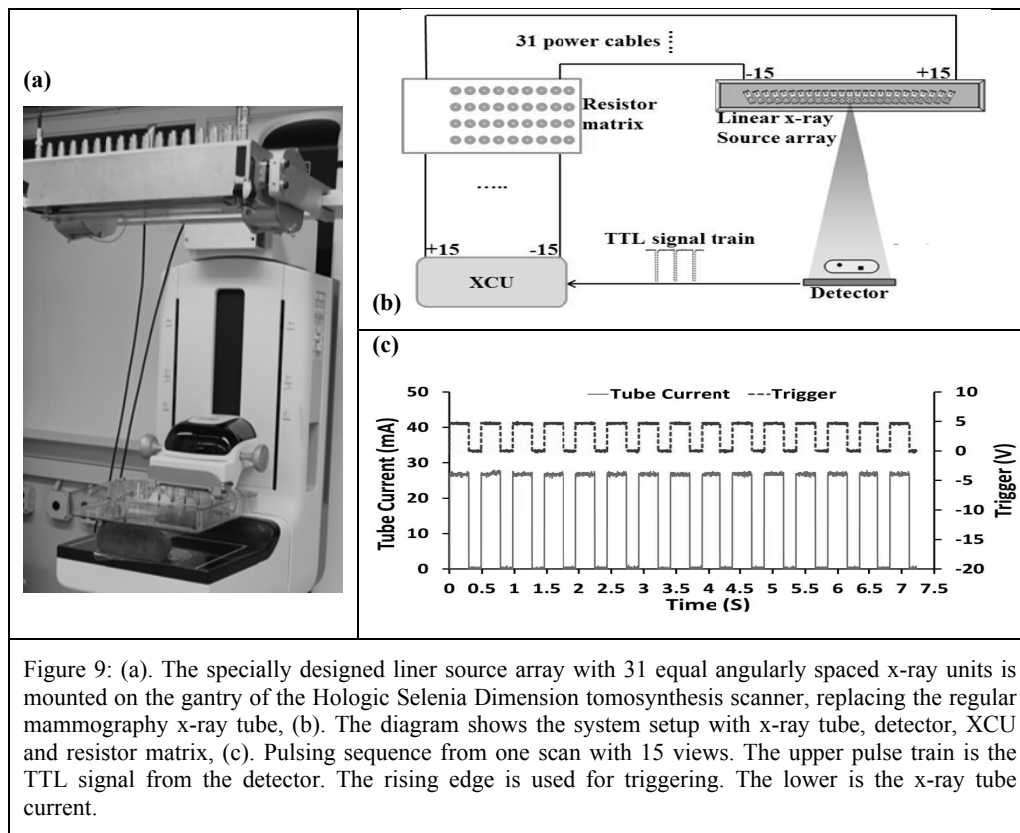
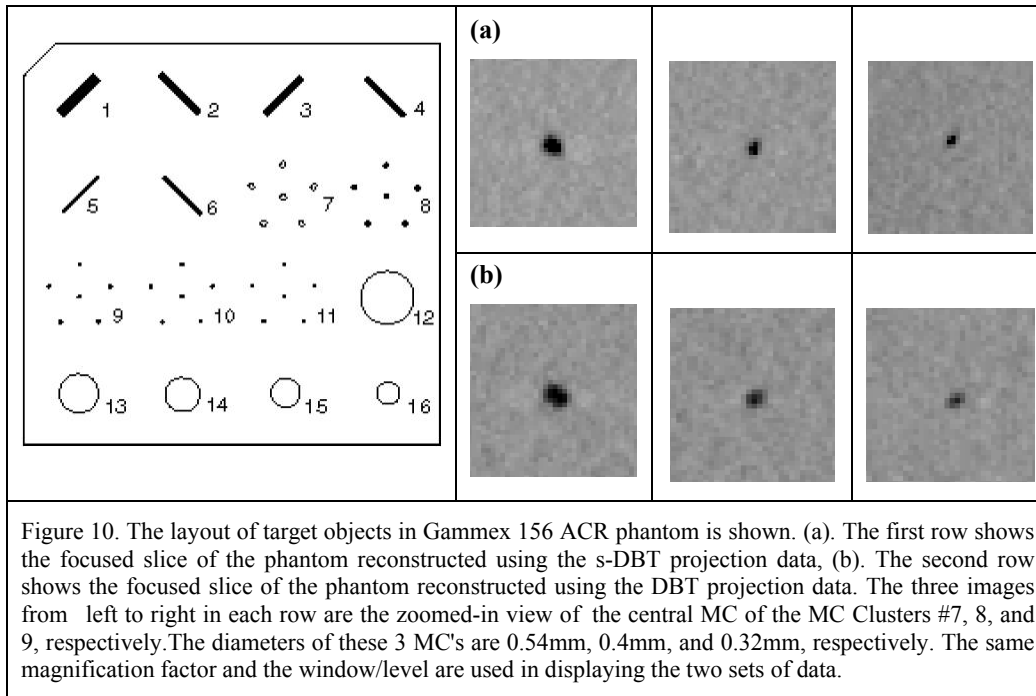


Figure 9: (a). The specially designed liner source array with 31 equal angularly spaced x-ray units is mounted on the gantry of the Hologic Selenia Dimension tomosynthesis scanner, replacing the regular mammography x-ray tube, (b). The diagram shows the system setup with x-ray tube, detector, XCU and resistor matrix, (c). Pulsing sequence from one scan with 15 views. The upper pulse train is the TTL signal from the detector. The rising edge is used for triggering. The lower is the x-ray tube current.

3.5 Initial phantom imaging

Fifteen projection images over 14 degrees angular span were collected using the s-DBT scanner and original Hologic Dimensions scanner with 28KVp anode voltage and 100mAs exposure level. The layout of target objects in Gammex 156 ACR phantom is shown in Figure 10. For comparison, the first row (a) and the second row (b) in Figure 10 show a focused slice of the ACR phantom reconstructed using the data collected from the s-DBT and the DBT system, respectively. The three images from left to right in each row are the zoomed-in view of the central MC of the MC Clusters #7, 8, and 9, respectively. The diameters of these 3 MC's are 0.54mm, 0.4mm, and 0.32mm, respectively. The same magnification factor and the window/level are used in displaying the two sets of data. Qualitatively the images in the first row collected using the s-DBT system is clearer.



4. DISCUSSION

In this article, we have demonstrated the feasibility of our new developed s-DBT scanner. A CNT cathode of 2.5x13mm rectangular shape was determined after electron optics simulation and careful considerations of emission area needed to get high current as well as sustainability of thermal loading by the anode. Given certain size of focal spot on anode, the heat load on anode increases accordingly with the increase of output exposure level. To maintain sufficient output exposure level for imaging, it is essential to keep heat load on anode within certain range (tungsten melting point is 3400°C). The anode heat dissipation ability showed in our thermal simulation allows us to have a higher tube current with the same FSS. In addition, based on the emission stability data from the current study and, we believe higher current can be achieved without enlarging the cathode size and therefore the FSS.

For the s-DBT scanner, the scanning time (t_{scan}) is determined by multiple factors including the number of views (N_{view}), detector readout time ($t_{readout}$), integration time ($t_{integration}$), total imaging exposure value (D_{total}), and x-ray tube current (I_{tube}). If the detector frame rate is not a limiting factor, then the scanning time can be calculated by: $t_{scan} = N_{view} \times (t_{readout} + D_{total} / (N_{view} \times I_{tube}))$. Assuming 100mAs is the total imaging exposure value distributed evenly over the 15 beams, the relation becomes: $t_{scan} = 15 \times (t_{readout} + 100 / (15 \times I_{tube}))$. The relation between the scanning time and tube current is plotted in Figure 11. The objective scanning time in this study is 6s without motion blurring. With 240ms detector readout time, using the tube current of 27mA, scanning time can be as fast as 6s for the total imaging dose of 100mAs. This value is slightly slower than the reported scanning times of Hologic DBT scanners (4s). Further reducing the scanning time can be achieved by either a detector with fast frame rate and higher tube current. For example, with 17ms detector readout time, if $I_{tube} = 38$ mA then t_{scan} becomes 3s. With the increase of angular coverage, the scanning time of Hologic scanner can be increased dramatically due to mechanical motion, while for s-DBT scanner the scanning time is about the same as the narrower angular coverage when detector readout time is 17ms.

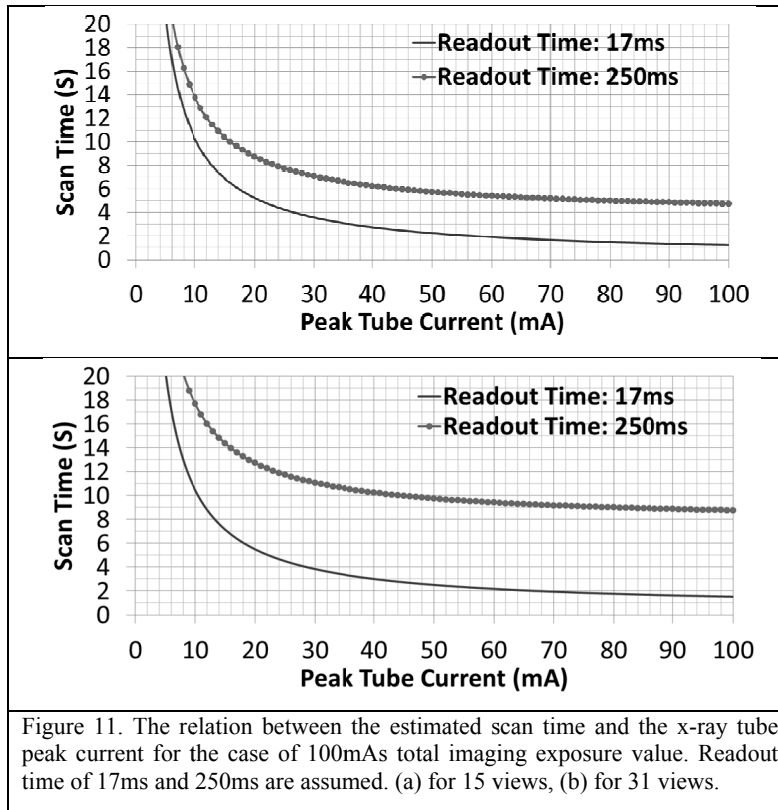


Figure 11. The relation between the estimated scan time and the x-ray tube peak current for the case of 100mAs total imaging exposure value. Readout time of 17ms and 250ms are assumed. (a) for 15 views, (b) for 31 views.

5. CONCLUSIONS

A prototype s-DBT scanner has been developed and evaluated by retrofitting the Hologic Selenia Dimension rotating gantry DBT scanner with a CNT field emission x-ray source array. These preliminary results demonstrate the feasibility and quality of the proposed s-DBT scanner. The initial reconstructed images using an ACR phantom show that s-DBT is fully functioning and can provide higher quality images. The scanning time depends on the detector speed and imaging configuration. At small angular coverage the s-DBT scanner is slower but becomes comparable and slightly faster than the rotating gantry system at larger coverage angles. The scanning time can be further reduced without sacrificing the resolution using a faster detector. Accelerated lifetime measurement demonstrated the long term stability of the CNT x-ray source array for digital breast tomosynthesis. The flexibility in configuration of the x-ray source array will also allow system designers to consider imaging geometries that are difficult to achieve with the conventional single-source rotating approach.

ACKNOWLEDGMENT

This research is currently supported by the following grants : NCI Grant No. U54CA119343, NIH R01 Grant No. CA134598-01 and the University Cancer Research Fund at the University of North Carolina. Dr. Xin Qian, is supported by a fellowship from DoD Grant No. BC087505.

REFERENCES

1. J.T. Dobbins III and D.J. Godfrey, *Digital x-ray tomosynthesis: current state of the art and clinical potential*. Phys. Med. Biol, 2003. **48**: p. R65-R106.
2. Poplack, S.P., et al., *Digital breast tomosynthesis: initial experience in 98 women with abnormal digital screening mammography*. American Journal of Roentgenology, 2007. **189**(3): p. 616.
3. Smith, A., et al. *Lesion Visibility in Low Dose Tomosynthesis*. in *International Workshop on Digital Mammography 2006*. 2006. Manchester, UK: Springer-Verlag Berlin Heidelberg 2006.
4. US-FDA, *Digital Accreditation*, U.D.O.H.H. Services, Editor 2011, <http://www.fda.gov/RadiationEmittingProducts/MammographyQualityStandardsActandProgram/FacilityCertificationandInspection/ucml14148.htm>.
5. Ren, B.R., et al., *A New Generation FFDM/Tomosynthesis Fusion System with Selenium Detector*. Proceeding of SPIE, 2010. **7622**: p. 11.
6. M. Bissonnette, et al. *Digital breast tomosynthesis using an amorphous selenium flat panel detector*. in *Medical Imaging 2005: Physics of Medical Imaging, Proceeding of SPIE Vol. 5745*. 2005.
7. Y. Zhang, et al., *A comparative study of limited-angle cone-beam reconstruction methods for breast tomosynthesis*. Med. Phys., 2006. **33**(10): p. 3781-3795
8. T. Wu, et al., *Tomographic mammography using a limited number of low-dose cone beam projection images*. Med. Phys, 2003. **30**(3): p. 369.
9. A. D. Maidment, et al., *Evaluation of a photon-counting breast tomosynthesis imaging system*. Proc. SPIE, 2006. **6142**: p. 89-99
10. Zhou, J., B. Zhao, and W. Zhao, *A computer simulation platform for the optimization of a breast tomosynthesis system*. Medical Physics, 2007. **34**(3): p. 1098-1108.
11. S.P. Poplack, et al., *Digital breast tomosynthesis: initial experience in 98 women with abnormal digital screening mammography*. AJR, 2007. **189**: p. 616.
12. P. Baldelli, et al., *A prototype of a quasi-monochromatic system for mammography applications*. Phys. Med. Biol, 2005. **50**: p. 2225-2240.
13. Baldelli, P., et al., *Dose comparison between conventional and quasi-monochromatic systems for diagnostic radiology*. Phys Med Biol., 2004. **49**: p. 4135-4146.
14. D.J. Crotty, R.L. McKinley, and M.P. Tornai, *Experimental spectral measurements of heavy K-edge filtered beams for x-ray computed mamotomography*. Phys. Med. Biol, 2007. **52**: p. 603.
15. R.L. Mckinley, et al., *Simulation study of a quasi-monochromatic beam for x-ray computed mamotomography*. Med. Phys, 2004. **31**(4): p. 800.
16. Baorui Ren, et al., *A new generation FFDM / tomosynthesis fusion system with selenium detector*. Medical Imaging 2010, Proc of SPIE 2010. **76220B-2**.
17. Xin Qian, et al., *Design and Characterization of a Spatially Distributed Multi-Beam Field Emission X-ray Source for Stationary Digital Breast Tomosynthesis* Medical Physics, 2009. **36**(10): p. 4389.
18. FDA, *Radiological Health-Performance Standards for Ionizing Radiation Emitting Products*, in 21, F.a.D. Administration, Editor 2010.
19. Carslaw, H.S. and J.C. Jaeger, *Conduction of Heat in Solids*1973: Oxford University Press.
20. IEC, *Medical electrical equipment –X-ray tube assemblies for medical diagnosis*, in *Characteristics of focal spots*2005: Geneva, Switzerland. p. 80.

Optimizing configuration parameters of a stationary digital breast tomosynthesis system based on carbon nanotube X-ray sources

Andrew Tucker*^a, Xin Qian^a, Emily Gidcumb^a, Derrek Spronk^b, Frank Sprenger^b, Johnny Kuo^c, Susan Ng^c, Jianping Lu^a, Otto Zhou^a

^aUniversity of North Carolina at Chapel Hill, Chapel Hill, NC, USA;

^bXinRay Systems LLC, Research Triangle Park, NC, USA;

^cReal-Time Tomography LLC, 1709 Balsam Lane, Villanova, PA, USA

ABSTRACT

The stationary Digital Breast Tomosynthesis System (s-DBT) has the advantage over the conventional DBT systems as there is no motion blurring in the projection images associated with the x-ray source motion. We have developed a prototype s-DBT system by retrofitting a Hologic Selenia Dimensions rotating gantry tomosynthesis system with a distributed carbon nanotube (CNT) x-ray source array. The linear array consists of 31 x-ray generating focal spots distributed over a 30 degree angle. Each x-ray beam can be electronically activated allowing the flexibility and easy implementation of novel tomosynthesis scanning with different scanning parameters and configurations. Here we report the initial results of investigation on the imaging quality of the s-DBT system and its dependence on the acquisition parameters including the number of projections views, the total angular span of the projection views, the dose distribution between different projections, and the total dose. A mammography phantom is used to visually assess image quality. The modulation transfer function (MTF) of a line wire phantom is used to evaluate the system spatial resolution. For s-DBT the in-plan system resolution, as measured by the MTF, does not change for different configurations. This is in contrast to rotating gantry DBT systems, where the MTF degrades for increased angular span due to increased focal spot blurring associated with the x-ray source motion. The overall image quality factor, a composite measure of the signal difference to noise ratio (SdNR) for mass detection and the z-axis artifact spread function for microcalcification detection, is best for the configuration with a large angular span, an intermediate number of projection views, and an even dose distribution. These results suggest possible directions for further improvement of s-DBT systems for high quality breast cancer imaging.

Keywords: Tomosynthesis, Mammography, CNT x-ray, Dose Distribution, Phantom Imaging, System

1. INTRODUCTION

Breast cancer is a life threatening disease that affects more than 200,000 women in the United States each year¹. Since 1990, breast cancer incidence rates for women in the United States have held constant, while mortality rates from breast cancer have steadily declined². The decline in mortality rates can largely be attributed to better mammography screening procedures. Current mammography practices use 2D imaging to screen women. Problems arise when underlying and overlying tissue obstruct the view of cancerous lesions in the breast. Digital Breast Tomosynthesis (DBT) uses multiple projection images over an angular span in order to create a 3D volumetric reconstruction of the breast³. This 3D reconstruction allows for lesions, which would otherwise be obscured from view, to become visible⁴.

Current DBT systems use a single x-ray source which is rotated over the angular span. Images are either taken during rotation or the system uses a "step and shoot" method^{5, 6}. Either method can result in blurring of the focal spot due to this motion. A blurred focal spot decreases the resolution of the system which can reduce microcalcification conspicuity. The "step and shoot" method has reduced focal spot blurring but at a cost of increased acquisition time⁷.

*awtucker@ncsu.edu; phone 1 919 962-3525; www.physics.unc.edu/project/zhou/

We have developed a prototype stationary digital breast tomosynthesis (s-DBT) system by retrofitting a Hologic Selenia Dimensions rotating gantry tomosynthesis system with a distributed carbon nanotube (CNT) x-ray source array^{8, 9, 10}. The system is capable of creating a full set of tomosynthesis projection images with no x-ray tube motion blurring and a decreased acquisition time.

The overall imaging performance of a DBT system depends on many factors including the x-ray source, the detector, the reconstruction and data processing methods, and the imaging configuration. There have been a large number of studies on how rotating gantry DBT system performance depends on the imaging configuration^{11, 12, 13}. The goal of this study is to investigate the relation between the performance of the CNT s-DBT system and its specific imaging configurations. The configuration variables include the total angular span, the number of projection views, the total dose, and the dose distribution across the projection images. Analysis was completed on reconstructed physical phantom images using quantitative measures including signal difference to noise ratio (SdNR), and Z-axis artifact spread function (ASF) analysis. Further analysis was conducted on the reconstructed images of a tungsten crosswire phantom by determining the modulation transfer function.

2. METHODOLOGY

2.1 CNT x-ray source array

The CNT x-ray source array consists of 31 individual x-ray generating focal spots in a linear array design⁹. The x-ray beam from each focal spot is independently controlled by the corresponding CNT field emission cathode. The electron beam is generated by applying an extraction voltage, approximately -1400V, between the cathode and the gate electrode. The tube is setup so that a constant kVp can be applied to the anode. The effective energy spectrum is determined by the sum of the anode and cathode voltages. Each x-ray beam can be instantaneously turned on/off by controlling the cathode-gate voltage. An electronic control system (ECS) was designed to produce constant tube current (< 1% fluctuation) over the lifetime of the tube operation. The anode material is tungsten and the x-ray window is 1 mm thick aluminum. The tube can be operated reliably at up to 50 kVp, with a potential lifetime up to 3 years in clinical operations⁹.

2.2 S-DBT system

The CNT x-ray source array is mounted on a commercial Hologic Selenia Dimensions DBT system (Hologic Inc.), in which the standard rotating anode mammography x-ray source has been removed. The detector for the system is 3328 by 4096 pixels with a pixel size of 0.07 mm. All tomosynthesis projection images are obtained in 2x2 binning mode making the effective pixel size 0.14 mm⁵. Figure 1 shows the Hologic system before and after integration with the CNT x-ray source.

2.3 Image acquisition configurations

Two physical phantoms were used to assess the image quality of the s-DBT system and its dependence on the acquisition configurations. The standard American College of Radiology (ACR) mammography accreditation phantom (CIRS Model 015) was imaged to assess the SdNR of masses and z-resolution sensitivity of microcalcifications. The ACR phantom contains aluminum oxide (AL₂O₃) specks ranging from 0.54 mm to 0.16 mm in diameter, masses ranging from 2 mm to 0.25 mm in thickness, and nylon fibers that range from 1.56 mm to 0.4 mm in diameter. Figure 2 shows a reconstructed volume slice of the ACR phantom using the s-DBT system. In addition to the ACR phantom, a homemade wire phantom consisting of 0.05 mm diameter tungsten wires was used to assess the MTF. All images were acquired using an effect potential difference of 31.4 kVp. The angular span, anode current, and number of projections views were determined by the particular configuration that was used.

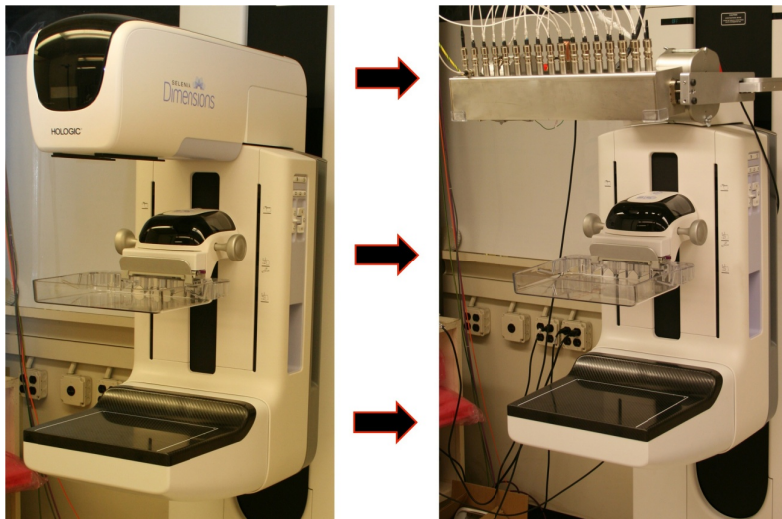


Figure 1. Left: Hologic Selenia Dimensions Digital Breast Tomosynthesis system with single rotating x-ray source, Right: stationary Digital Breast Tomosynthesis system with integrated CNT based distributed source array. There are 31 x-ray generating focal spots; each x-ray beam can be electronically controlled to turn on/off instantaneously.

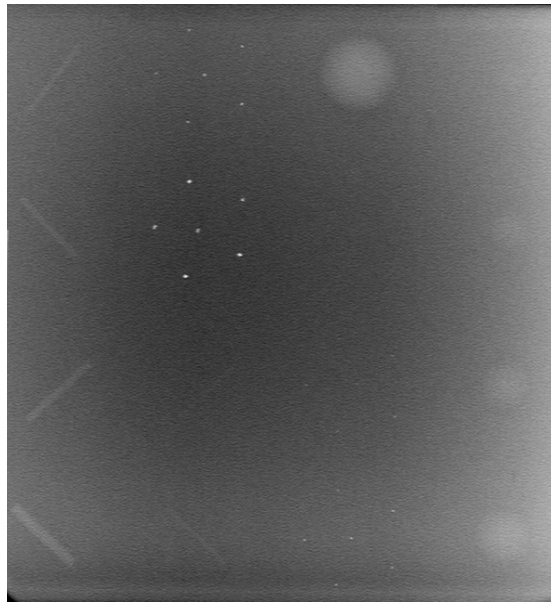


Figure 2. ACR phantom image acquired using our s-DBT system. The phantom contains simulated masses, microcalcifications, and fibers. Analysis was conducted on the masses and microcalcifications

The quality of tomosynthesis images can depend on many factors such as the angular span of the projection images, the number of projection views, the total dose and dose distribution, the detector resolution and sensitivity, and the reconstruction algorithm. Here we concentrated on the variation of geometry parameters and dose. The same reconstruction method (see section 2.4) and detector was used for all imaging configurations.

Four groups of comparison studies were done: (1) For a fixed dose of 100 mAs and 15 projection views, we compare the angular span of 14° versus 28° ; (2) For a fixed dose of 100 mAs and an angular span of 28° , we compare 15 versus 29 projection views; (3) For a fixed total dose of 100 mAs an angular span of 28° and 29 projection views, we compare three different dose distributions; (4) For a fixed angular span of 28° and 29 projection views, we vary the total dose from 60 mAs to 120 mAs. All configurations are listed in Table 1.

Table 1. List of Configurations and parameters that were analyzed. Four parameters were changed in order to create different configurations; number of projection views, total angular span, total dose, and dose distribution. Some configurations appear in more than one group.

Group	Number of Projections	Total Angular Span	Angular Spacing	Total Dose (mAs)	Dose Distribution
1	15	14°	1°	100	Equal dose on all projections
1	15	28°	2°	100	Equal dose on all projections
2	15	28°	2°	100	Equal dose on all projections
2	29	28°	1°	100	Equal dose on all projections
3	29	28°	1°	100	Equal dose on all projections
3	29	28°	1°	100	1/3 total dose on central 15 projections; 2/3 total dose on exterior 14 projections
3	29	28°	1°	100	2/3 total dose on central 15 projections; 1/3 total dose on exterior 14 projections
4	29	28°	1°	60	Equal dose on all projections
4	29	28°	1°	80	Equal dose on all projections
4	29	28°	1°	100	Equal dose on all projections
4	29	28°	1°	120	Equal dose on all projections

2.4 Image processing and reconstruction

For each configuration a set of blank images were acquired. Dark images were acquired for the two detector integration times that were used, 274 ms and 295 ms. Projection images of the ACR and wire phantom were processed using Equation 1. This processing helps correct for detector and beam non-uniformity as well as gain offsets.

$$Image = \frac{Projection - Dark}{Blank - Dark} \quad (1)$$

Reconstruction of the 3D volume was completed using a dynamic 3D reconstruction software package developed by Real Time Tomography, LLC (Villanova, PA). This software uses a back projection filtering method¹⁴. The reconstructed volumes have a pixel size of 0.1 mm at the focal plane and a distance between slices of 0.5 mm.

2.5 SdNR analysis

The ability of a DBT system to detect masses in the breast is primarily determined by in-plane contrast. Signal difference to noise ratio (SdNR) is a measure of the contrast with respect to the noise level. SdNR analysis was completed on the 2 mm mass that is embedded in the ACR phantom. The foreground was selected to be the mass and the background was selected to be a circular region surrounding the mass.

To determine the noise in the foreground and background, a moving average filter was used across the original image and the resultant image was subtracted from the original. This is used to remove systematic variation of the background image that is not due to noise. The standard deviation was taken of the two regions in the subtracted image.

Equation 2 shows the calculation used to determine the SdNR of the images. In the equation “ μ_{signal} ” and “ μ_{bkg} ” signify the average pixel intensity of the foreground and background respectively. The variables “ σ_{signal} ” and “ σ_{bkg} ” signify the standard deviation of the subtracted foreground and background image respectively⁷.

$$SdNR = \frac{|\mu_{signal} - \mu_{bkg}|}{\sqrt{0.5 * (\sigma_{signal}^2 + \sigma_{bkg}^2)}} \quad (2)$$

2.6 Z-axis artifact spread function analysis

The depth resolution of DBT can be measured by the z-axis artifact spread function (ASF). The AFS was calculated for the 0.54 mm aluminum oxide specks. These specks are used to simulate microcalcifications (MC) which can be a precursor to breast cancer. There are a cluster of six specks in the phantom and the analysis was completed on the central speck. Due to the small size of the MC it is difficult to determine the average pixel intensity value of the speck. We calculated the ASF by taking the maximum pixel value found in a small region of interest (ROI), where the central speck would be, through every reconstruction slice of the reconstruction space⁷. Each reconstruction slice is located 0.5 mm above the previous slice. As the distance from the current slice becomes farther from the focus plane of the specks the intensity of the ASF decreases. We use the width of the ASF at the 50% peak value as a quantitative measure of the z-axis spatial resolution.

Equation 3 shows the calculation used to determine the ASF. In the equation “i” is the current reconstruction slice, “max (signal(i))” is the maximum pixel value of the ROI of the current reconstruction slice, and “ $\mu_{bkg}(i)$ ” is the average value of the background of the current reconstruction slice⁷. Once the ASF was calculated the data was fitted to two Gaussian functions before the value at 50% was determined.

$$ASF(i) = \frac{|\max (signal(i)) - \mu_{bkg}(i)|}{\mu_{bkg}(i)} \quad (3)$$

2.7 MTF calculation

Using the 0.5 mm crosswire phantom the system Modulation Transfer Function was calculated. We used a method of MTF calculation that was previously published¹⁵. Using an oversampled line spread function we fitted the data to a Gaussian function. The Fourier transform of the fitted Gaussian function is the MTF. The spatial resolution at 10% MTF peak value is used as the quantitative measure of the in-plane image resolution.

2.8 Image quality factor

To assess the overall performance of the s-DBT system in detecting both the mass and MC we use the composite measure of image “quality factor” (QF). Equation 4 shows the calculation we used for the quality factor. It is similar in scope to a previously published method¹³. In the equation “SdNR” is the value determined from the signal difference to noise ratio calculation and “ASF” is the width of the artifact spread function at 50%.

$$QF = \frac{SdNR}{ASF} \quad (4)$$

3. RESULTS

Data was collected for the SdNR, the width of the ASF at 50%, and the MTF at 10% for each configuration. A summary of the results for all configuration studies is shown in Table 2.

Table 2. Calculated results for SdNR, ASF at 50%, and MTF. Data is separated into the four groups of configurations that were outlined in section 2.3. The configuration with 15 projection views, a 28 degree angular span, and an even dose distribution resulted in the highest “quality factor” value.

Group	Number of Projections	Angular Span	Total Dose (mAs)	Dose Distribution	SdNR	ASF at 50% (mm)	MTF (lp/mm)	QF
1	15	14°	100	Equal dose	5.28	8.42	4.12	0.627
1	15	28°	100	Equal dose	5.06	4.18	4.13	1.211
2	15	28°	100	Equal dose	5.06	4.18	4.13	1.211
2	29	28°	100	Equal dose	5.25	4.69	4.22	1.120
3	29	28°	100	Equal dose	5.25	4.69	4.22	1.120
3	29	28°	100	Lower on central; Higher on exterior	4.69	4.85	4.2	0.967
3	29	28°	100	Higher on central; Lower on exterior	4.87	4.19	4.23	1.161
4	29	28°	60	Equal dose	3.73	4.91	4.28	0.760
4	29	28°	80	Equal dose	4.35	4.68	4.25	0.930
4	29	28°	100	Equal dose	5.25	4.69	4.22	1.120
4	29	28°	120	Equal dose	5.76	4.82	4.21	1.196

3.1 SdNR

A magnified image of the ACR phantom mass which was used in the calculation of the SdNR is shown in Figure 3. Looking at table 2 it can be seen that the SdNR did not fluctuate greatly when the angular span was increased (Group 1). This was expected since the only differences in photon counts were the slightly higher source to object distance for the wider angular span. When the number of projection images was increased the SdNR did not change drastically (Group 2). Group 3 had different dose distributions with the same total dose. A lower SdNR was found in the configurations that had non-uniform distributions. This can be attributed to the lower photon count on some of the projection images of the uneven dose distributions. When the total dose was increased (Group 4) there was a corresponding increase in SdNR. The increased photon count gave a much larger signal difference which contributed to the increased SdNR.

3.2 MTF

The value at 10% of the MTF was used as a quantitative measure of in-plane resolution. Figure 4 shows an example of one of the line spread functions and the corresponding MTF.

As can be seen in Table 2, there was no significant change in the value of the MTF at 10% for the different configurations. This is because the in plane resolution is predominately determined by focal spot size and the detector pixel size. Since there is no focal spot blurring in s-DBT for different configurations, the MTF does not change. This is in contrast to a rotating gantry DBT, in which a large angular span or a large number of projection views can lead to large focal spot blurring associated with x-ray source motion or mechanical instability, thus degrading the MTF. The 10% MTF system resolution in s-DBT is found to be significantly higher than that of a typical DBT system¹⁰.

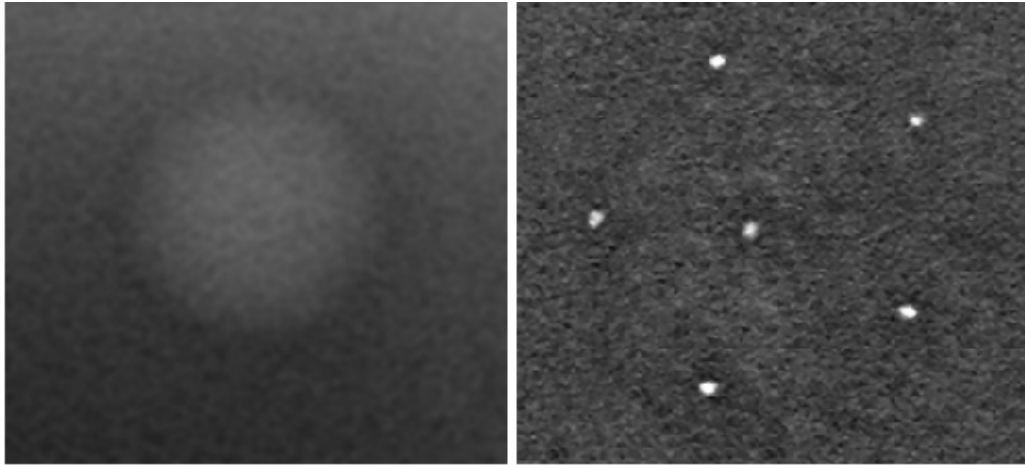


Figure 3. Left: Magnified view of 2 mm mass found in the ACR phantom. The SdNR of the mass and the surrounding background was calculated for each configuration. Right: Magnified view of the 0.54 mm speck cluster found in the ACR phantom. ASF analysis was completed on the central speck in the cluster for each configuration.

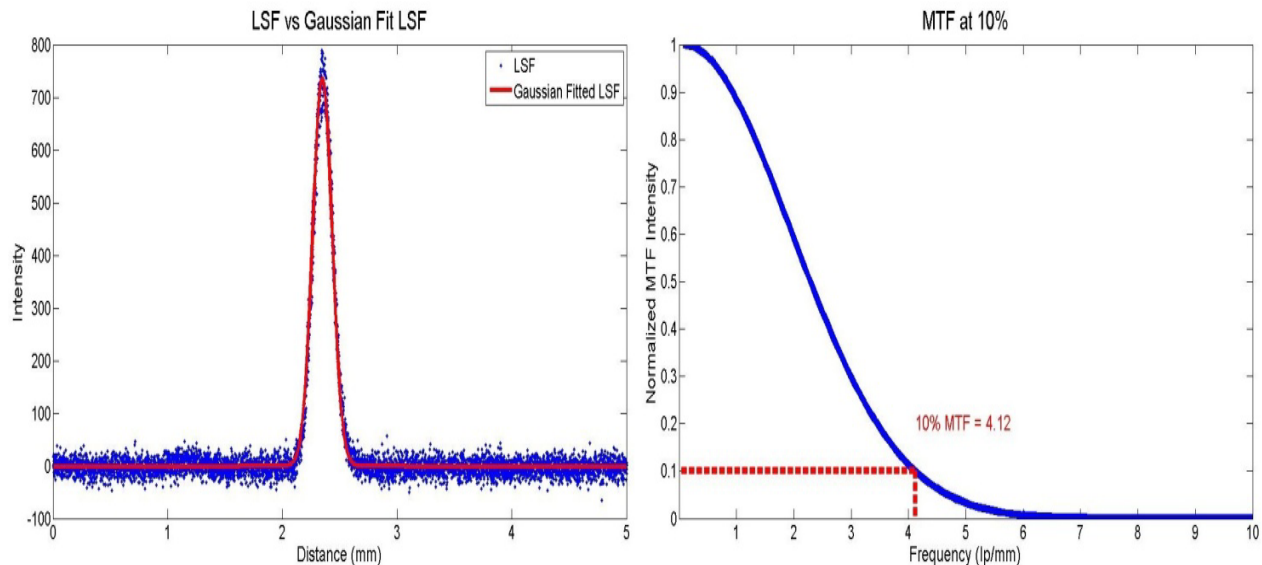


Figure 4. Left: Plot of the oversampled LSF and the corresponding Gaussian fitted LSF which was used for MTF calculations. Right: MTF of the LSF with the value at 10% highlighted. The MTF was found to be around 4.2 line pairs per mm for each configuration. There was no significant change in MTF value for the different configurations.

3.3 Artifact spread function

A magnified image of the ACR phantom speck cluster, which was used in the calculation of the artifact spread function, can be found in Figure 3. The central speck is used for quantitative analysis of the ASF for all configurations. As can be seen in Table 2 and Figure 5, there is dramatic change in ASF going from 14 degree to 28 degree angular span. This trend can be clearly seen in Figure 6 where the width at 50% ASF is plotted versus the total angular span ranging from 8 to 28 degrees. The apparent decrease of the width of the ASF can be attributed to the increased information which is collected in the projection space when the angular span is increased. Similar results have been found in previous studies^{11, 12}. For a fixed angular span, the ASF is found to be insensitive to the number of projection views, the total dose, and dose distribution.

3.4 Optimal configuration as determined by the image quality factor

The image quality factor is helpful in evaluating which configuration is better overall when taking into account both the ASF and SdNR. The QF equation only takes into account the SdNR and ASF because the MTF was found not to be affected by the change in configuration parameters. As table 2 shows the QF, for a given fixed dose and angular span, is similar for uniform and non uniform dose distribution over the fixed number of projection views (Group 3). The QF is clearly better for a large angular span versus a smaller one (Group 1). Though the QF for 15 and 29 views (Group 2) are similar for a given angular span, due to the finite detector frame rate the scanning time for 29 views is significantly longer. Thus, we conclude that overall the best configuration is the one with 28 degree angular span and 15 projection views with uniform dose distribution.

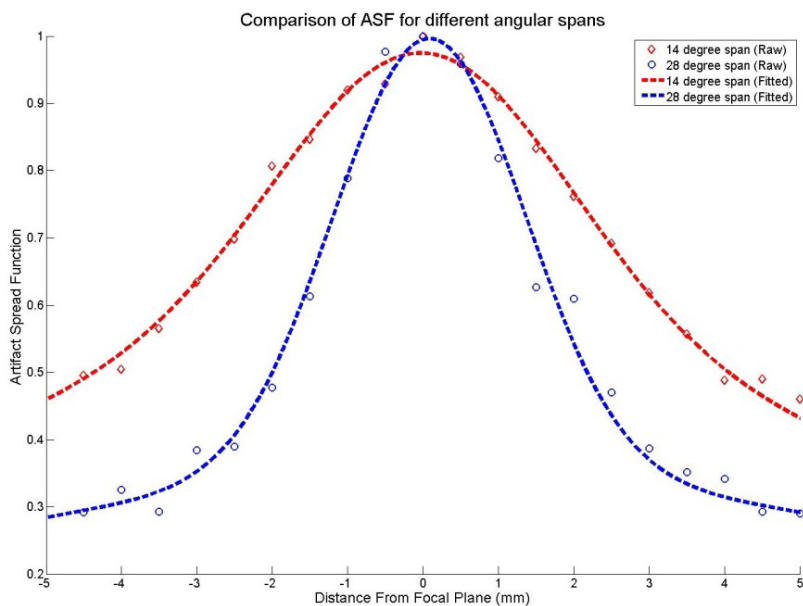


Figure 5. Comparison of the ASF of an angular span of 14 degrees versus an angular span of 28 degrees. Both the raw data and the data fitted to two Gaussian functions are shown. The 14 degree span resulted in a much broader ASF due to the lack of information in the projection space.

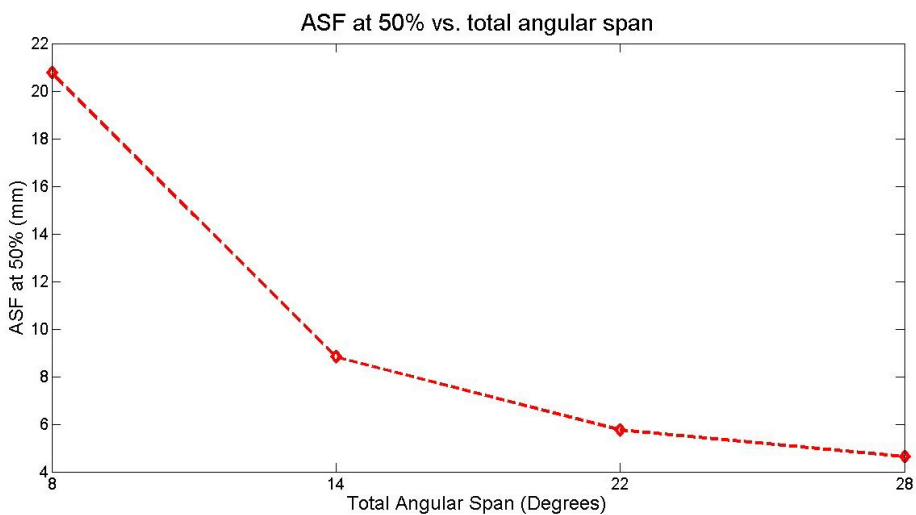


Figure 6. Results showing the effect of total angular span on the width of the ASF at 50%. A very noticeable trend can be seen which shows that an increased angular span results in a better artifact spread function.

4. DISCUSSION AND CONCLUSIONS

We have evaluated how the image quality of reconstructed data sets from our s-DBT system depends on parameters including the number of projection images, angular span, and dose distribution. The modulation transfer function did not fluctuate between the different configurations. This is due to the fact that it is more heavily dependent on the focal spot size, pixel size, object magnification, and the reconstruction algorithm used. However, in current DBT systems which utilize continuous motion in order to reduce acquisition time the MTF degrades due to the motion blur of the focal spot¹⁰. Therefore, different configurations would result in different MTF values. The s-DBT system has no focal spot blurring so the MTF does not degrade even when different configurations are used.

Adding extra projections to the configuration did not affect the quality of the images significantly. However, as the angular span increased the z-axis resolution increased. The increased z-axis resolution could be very beneficial when imaging patients since there will be tissue around the object of interest that the viewer would not want to obscure their view. Increased angular range becomes a problem for current DBT systems due to the increased focal spot blurring and/or acquisition time¹⁰.

As the total dose increased the SdNR also increased. When determining the total dose it is best to determine a dose for the patient that will have enough photons penetrate to the detector while keeping in mind that over dosing could be harmful to patients. The distribution of the dose did not have a large effect on the overall quality of the images. But a better SdNR was observed in the even distribution. It was found that a configuration with a large angular span, an intermediate number of projection views, and an even dose distribution resulted in the best overall image quality.

5. ACKNOWLEDGMENTS

The project is supported by the National Cancer Institute under grant number U54CA119343 and R01CA134598. We thank Hologic for providing the Selenia Dimensions Tomosynthesis System and for technical support.

REFERENCES

- [1] <http://www.cancer.gov/cancertopics/types/breast>
- [2] <http://www.cancer.gov/aboutnci/servingpeople/snapshots/breast.pdf>
- [3] Dobbins, J.T., "Tomosynthesis imaging: At a translational crossroads," *Med Phys* 36, 1956-67 (2009).
- [4] Andersson, I., Ikeda, D. M., Zackrisson, S., Ruschin, M., Svahn, T., Timberg, P., and Tingberg, A., "Breast tomosynthesis and digital mammography: a comparison of breast cancer visibility and BIRADS classification in a population of cancers with subtle mammographic findings", *Eur Radiol* 18, 2817-2825 (2008).
- [5] Ren, B., Ruth, C., Wu, T., Zhang, Y., Smith, A., Niklason, L., Williams, C., Ingal, E., Polischuk, B., and Jing, Z., "A new generation FFDM/tomosynthesis fusion system with selenium detector", *Proc. SPIE* 7622, 76220B (2010).
- [6] Eberhard, J. W., Albagli, D., Schmitz, A., Claus, B. E. H., Carson, P., Goodsitt, M., Chan, H. P., Roubidoux, M., Thomas, J. A., and Osland, J., [Lecture Notes in Computer Science -- Digital Mammography], Springer-Verlag, Manchester UK, 137-143 (2006).
- [7] Shaheen, E., Marshall, N., and Bosmans, H., "Investigation of the effect of tube motion in breast tomosynthesis: continuous or step and shoot?", *Proc. SPIE* 7961, 79611E (2011).
- [8] Qian, X., Rajaram, R., Calderon-Colon, X., Yang, G., Phan, T., Lalush, D., Lu, J., and Zhou, O., "Design and characterization of a spatially distributed multibeam field emission x-ray source for stationary digital breast tomosynthesis", *Med. Phys.* 36, 4389-4399 (2009).
- [9] Sprenger, F., Spronk, D., Calderon, X., Gidcumb, E., Lu, J., Qian, X., Tucker, A., Yang, G., and Zhou, O., "Stationary digital breast tomosynthesis with distributed field emission x-ray tube", *Proc. SPIE* 7961, 796151 (2011).
- [10] Qian, X., Tucker, A., Gidcumb, E., Shan, J., Yang, G., Calderon-Colon, X., Sultana, S., Lu, J., and Zhou, O., "High Resolution Digital Breast Tomosynthesis Using Distributed Carbon Nanotube X-Ray Source Array", Submitted to *Med. Phys.*, (2011).
- [11] Zhao, B., Zhou, J., Hu, Y. H., Mertelmeier, T., Ludwig, J., and Zhao, W., "Experimental validation of a three-dimensional linear system model for breast tomosynthesis", *Med. Phys.* 36(1), 240-251 (2009).
- [12] Chawla, A. S., Lo, J. Y., Baker, J. A., and Samei, E., "Optimized image acquisition for breast tomosynthesis in projection and reconstruction space", *Med. Phys.* 36(11), 4859-4869 (2009).

- [13] Sechopoulos, I., and Ghetti, C., "Optimization of the acquisition geometry in digital tomosynthesis of the breast", *Med. Phys.* 36(4), 1199-1207 (2009).
- [14] Kuo, J., Ringer, P. A., Fallows, S. G., Bakic, P. R., Maidment, A. D. A., and Ng, S., "Dynamic reconstruction and rendering of 3D tomosynthesis images", *Proc. SPIE* 7961, 796116 (2011).
- [15] Kwan, A. L. C., Boone, J. M., Yang, K., and Huang, S. Y., "Evaluation of the spatial resolution characteristics of a cone-beam breast CT scanner", *Med. Phys.* 34, 275-281 (2007).

Stationary Digital Tomosynthesis System for Early Detection of Breast Tumors

Background:

Digital breast tomosynthesis (DBT) is a limited angle computed tomography technique that can distinguish tumors from its overlying breast tissues and has potentials for detection of cancer at earlier stage. Current prototype DBT scanners are based on the regular full-field digital mammography systems and require partial isocentric motion of an x-ray tube over certain angular range to record projection views. This prolongs the scanning time and in turn degrades the imaging quality due to motion blur. To mitigate the above limitations, a stationary DBT (s-DBT) scanner has been recently developed in our lab.

Methods:

The proposed s-DBT scanner uses the carbon nanotube (CNT) based spatially distributed multi-beam field emission x-ray (MBFEX) technology. The system records all the projection images by electronically activating the multiple x-ray beams from different viewing angles without any mechanical motion.

Results:

31 individually controllable x-ray beams for the proposed s-DBT scanner has been designed and characterized. The experimental study showed promising results. The scanning time is as short as 4 seconds with output exposure level of 100mAs. The measured focal spot size (FSS) is 0.7x0.6mm using 2.5x13mm rectangular CNT cathodes. Both of scanning time and FSS are superior to the latest DBT systems from commercial vendors. The other preliminary results in term of x-ray source stability showed that the CNT based MBFEX source can be operated for at least 7 years for a busy mammography clinic.

Conclusions:

These preliminary results demonstrate the feasibility of the proposed s-DBT scanner. The technology has the potential to increase both the temporal and spatial resolution, simplify the system design, and reduce the scanning time.

